TECHNISCHE UNIVERSITÄT
CHEMNITZ

Fakultät für Informatik

CSR-26-04

GPS-based UAV Precision Landing

Atul Chandra Nath · Reda Harradi · Wolfram Hardt

April 2026

Chemnitzer Informatik-Berichte

TECHNISCHE UNIVERSITÄT
CHEMNITZ

GPS-based UAV Precision Landing

Master Thesis

Submitted in Fulfilment of the
Requirements for the Academic Degree
M. Sc. Automotive Software Engineering

Dept. of Computer Science
Chair of Computer Engineering

Submitted by: Atul Chandra Nath
Date: 19.03.2026

Supervising tutors: Prof. Dr. Dr. h. c. Wolfram Hardt
Reda Harradi, M.Sc.

Abstract

Unmanned Aerial Vehicles, also known as UAVs, are used in various fully autonomous use cases, such as product delivery, inspection of infrastructure, or, in the case of an emergency, like a search and rescue mission. When standard GPS-based positioning is used, it provides meter-level accuracy, which is not sufficient in the case of autonomous landing. This thesis focuses on RTK or Real-Time Kinematic-based positioning in order to achieve centimeter-level accuracy at the time of landing, including the evaluation of hardware, system integration, and both local and real-world correction services.

This thesis presents a systematic study of multiple U-blox GNSS devices, such as Ardusimple Simplertk2B devices, which have both ZED-F9P and ZED-F9R, and Here+ RTK M8P. These devices are then integrated using a Pixhawk flight controller running ArduPilot firmware to work as a base and rover interchangeably, in order to assess whether different GNSS modules can be used without significant performance reduction. We have tested both our locally set-up base station and the real-world SAPOS network-based correction service to check the integrity of our system.

This thesis describes in detail our system architecture, different GNSS configurations based on system requirements, and Pixhawk integration. Based on this setup, we have monitored our system in both the indoor(semi-obstructed) laboratory and the open-sky outdoor environment to test the impact of the environment on the positional accuracy. The findings from the experiment suggest that in open-sky conditions, horizontal accuracy is at the centimeter-level and below 2 cm of 3D positional accuracy which was achieved by the ZED-F9P under favorable RTK-fix conditions, whereas in the worst case, meter-level errors can be observed. This thesis concludes with a detailed discussion of our system limitations and explores future directions, such as GNSS-vision fusion and advanced RTK techniques.

Keywords: UAV Precision Landing, RTK GNSS, GNSS Accuracy, Pixhawk Integration, SAPOS Correction Service

Acknowledgment

I want to extend my sincere thanks to Prof. Dr. Dr. h.c. Wolfram Hardt, Chair of the Computer Engineering of Faculty of the Computer Science department at the Technische Universität Chemnitz. His cordial efforts to organize and provide every Master's student of Automotive Software Engineering course with the chance to gain a practical, industry-like experience during the thesis process. His Thesis Master class helped me a lot to understand every step of the thesis process, from planning the thesis to writing the final report.

A special gratitude goes to my thesis supervisor, Mr. Reda Harradi, for his incredible support and continuous guidance during my thesis journey. His valuable advice, continued encouragement, insightful guidance during the experimental data collection helped me to successfully complete my thesis. I also appreciate him for sharing his valuable knowledge with me in every phase of the thesis.

Finally, i would like to show my deepest gratitude to my family and friends, who have given immense support during my study.

Table of Contents

List of Figures

List of Tables

List of Abbreviations

GNSS	Global Navigation Satellite System
GPS	Global Positioning System (USA)
GLONASS	Globalnaya Navigatsionnaya Sputnikovaya Sistema (Russia)
Galileo	European Global Navigation Satellite System
BeiDou	BeiDou Navigation Satellite System (China)
PNT	Positioning, Navigation, and Timing
RTK	Real-Time Kinematic
NRTK	Network Real-Time Kinematic
DGPS	Differential Global Positioning System
SBAS	Satellite-Based Augmentation System
UTC	Coordinated Universal Time
DOP	Dilution of Precision
GNSS/INS	GNSS and Inertial Navigation System Integration
3D Fix	Three-Dimensional Position Fix
RTK Float	Real-Time Kinematic Floating Ambiguity Solution
RTK Fixed	Real-Time Kinematic Fixed Ambiguity Solution
LAMBDA	Least-squares AMBiguity Decorrelation Adjustment
SAPOS	Satelliten-positionierungsdienst der deutschen Landesvermessung
HEPS	Hochpräziser Echtzeit-Positionierungs-Service
VRS	Virtual Reference Station
MAC	Master-Auxiliary Concept
FKP	Flächenkorrekturparameter (Area Correction Parameter)
NTRIP	Networked Transport of RTCM via Internet Protocol
RTCM	Radio Technical Commission for Maritime Services
UBX	u-blox Proprietary Binary Protocol
PVT	Position, Velocity, and Time
SVIN	u-blox Survey-In (UBX-NAV-SVIN)
UBX-CFG	u-blox Configuration Message Class
UBX-MON	u-blox Monitoring Message Class (e.g., UBX-MON-VER)
NMEA	National Marine Electronics Association (Standard Protocol)
TMODE3	Timing Mode 3 (Survey-in or Fixed Mode for Base Stations)
UAV	Unmanned Aerial Vehicle

ZED-F9P	u-blox ZED-F9P Multi-Band GNSS RTK Receiver
H-RTK F9P	Holybro High-Precision GNSS RTK Module
ESP32	Espressif Systems Microcontroller
IMU	Inertial Measurement Unit
EMI	Electromagnetic Interference
UWB	Ultra-Wideband
JST-GH	Japan Solderless Terminal - Global Hybrid Connector
MAVLink	Micro Air Vehicle Link
IEEE 802.11	Wireless Local Area Network (Wi-Fi Standard)
UART	Universal Asynchronous Receiver-Transmitter
I2C	Inter-Integrated Circuit
SPI	Serial Peripheral Interface
USB	Universal Serial Bus
CAN	Controller Area Network
COM	Communication Port (Serial Port Interface)
TELEM1	Primary Telemetry Port
YOLO	You Only Look Once (Object Detection Algorithm)
API	Application Programming Interface
UUID	Universally Unique Identifier
PostgreSQL	Postgres Structured Query Language Database

1 Introduction

1.1 Background and Motivation

The development of unmanned aerial vehicles (UAVs) also known as drones has experienced rapid technological advancements in the recent years. The use of UAV's is getting common in commercial, industrial and research applications [1, 2]. With modern UAV systems required to perform autonomous operations in complex environments with limited or no human intervention; typical applications include parcel delivery, power-line and forest inspection[TUC1, TUC2], environmental monitoring and search-and-rescue missions [1] [TUC3] are well known. For most of these scenarios, an accurate and reliable landing capability is essential to the success or safety of these operations. Autonomous landing of UAV's is particularly challenging because it requires very accurate position estimation during the final stages of flight. Most standard global navigation satellite system (GNSS) positioning techniques will provide a level of accuracy of meters under open sky conditions, which is suitable for navigation purposes but not sufficient for precision landing operations where the landing point may be small like our hanger landing spot or encumbered with obstacles [3]. Even small positional errors can result in mission failure, damage to hardware and risk to people and property in densely populated or industrial areas.

Real-time kinematic (RTK) positioning can be used as a solution to address the current limitations of UAV navigation. RTK provides centimeter-level of accuracy using differential corrections that can be provided from either a single base station or through network correction services like SAPOS [4]. Advances in cost-effective, multi-frequency GNSS receiver technology and RTK enabled UAV platforms have greatly reduced the barriers for the adoption of RTK technology in UAV systems [5]. As a result, the research and industrial communities have been able to investigate high-accuracy navigation solutions for UAV's without reliance on expensive equipment.

Despite the advances made in recent years there are still significant challenges to be overcome prior to practical UAV deployment. As it requires robust integration of GNSS hardware, correction services, flight control systems and software frameworks. There can be some environmental factors occurs such as multi-path effects, signal blockages, and interference which can negatively impact positioning performance and accuracy in urban or semi-obstructed like environments [6], for example, our TUC drone lab which used as a semi-obstructed environment. For our case, we saw that signal quality impacted when devices are kept open sky vs. in semi-obstructed conditions. For this reason, a systematic evaluation of RTK based UAV landing systems is necessary to evaluate the suitability and scalability of these systems for operational use. This includes comparison of different types of GNSS hardware, analysis of different sources of correction data, and experimental evaluation of real world UAV landing performance [7, 8].

The objective of this thesis is to design, develop and experimentally evaluate a practical RTK based UAV positioning framework capable of providing support for precision landing operations in a variety of environmental conditions.For getting a brief idea of this thesis, We can consider the diagram 1 which is an example of precision landing representation of the geometric relationships that exist during a vertical descent of a UAV to a landing point. The position of the UAV relative to the landing mark, as well as the camera height, as can be seen on the left side of the diagram. And the right-hand side of the diagram

is an example of the UAV at an angle of tilt; it shows how variations in orientation will affect the projected location of the landing point for this specific landing area.

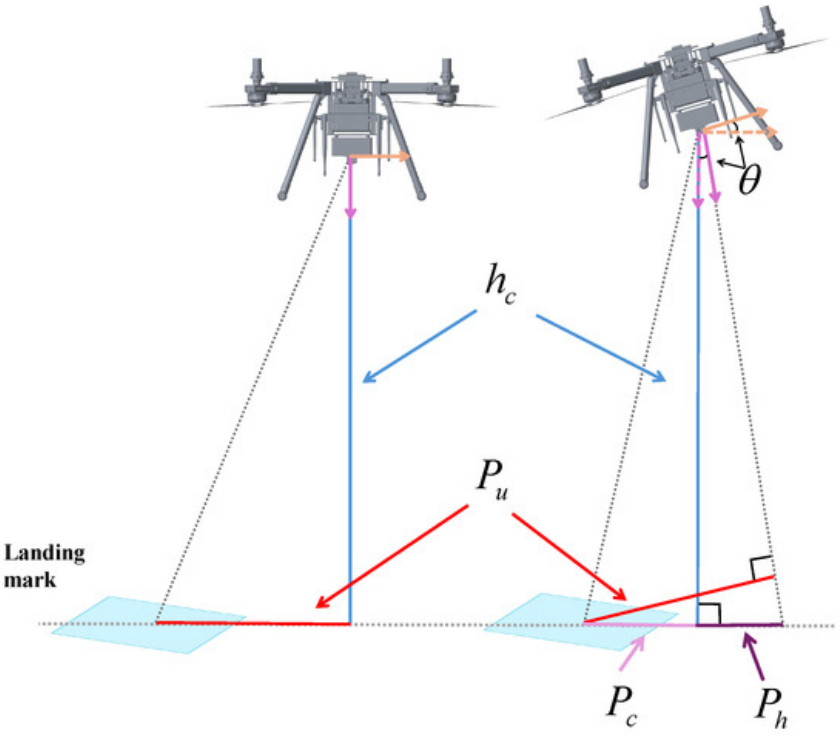

Figure 1: UAV landing geometry with attitude effects [11].

1.2 Problem Statement

Our study found that current conventional GPS-based UAV navigation systems can achieve a level of accuracy which is meter-level but do not meet the demands of precision landing on predetermined targets (such as charging pads, docking stations, or delivery platforms) [3]. For example, in case of our drone hanger system, accuracy should be below 2 cm for rover and the base also needs to be surveyed up-to below 0.5m in an ideal case in order to safe and precision landing, as the width and height of the landing area is below 2 meters. RTK GNSS based systems have theoretical capability to provide centimeter level accuracy. But the practical performance will depend on many variables including the quality of the receiver hardware, availability of corrections, reliability of communications, environmental conditions and overall system design and integration [4, 9].

After doing the theoretical study specifically in relation to the development of autonomous UAV infrastructure at the Professorship of Computer Engineering at Chemnitz University of Technology, some shortcoming were concretely observed. In particular, the operational decentralized UAV hangar that was developed as part of the RescueFly project for a defined landing area, automatic recharging of the batteries (after each flight), and a cloud-based architecture for MAVLink based control of the UAVs [TUC3, TUC4], does not specified any information about the precision landing controller or RTK solution quality monitoring or even a failure-handling procedure in the time of landing phase. the accuracy of landing for the current hangar system is 0.15 m which is compensated by a mechanical repositioning module that will be executed after the UAV has landed. For this

reason, there is a need for the development of a landing system to provide a failure-safe precision landing.

Current UAV implementations are primarily focused on one of two types of landing approaches, either vision-based systems or solely GNSS-based navigation without an overall assessment of combined RTK-based landing frameworks. There is limited comparison of the relative performance of various low cost GNSS modules utilizing interchangeable base-rover configurations along with multiple correction sources [10].

Therefore, a systematic study is required to evaluate the above mentioned key challenges:

- Combining low-cost RTK GNSS receivers with UAV flight controllers.
- Evaluating the positioning performance using different hardware platforms.
- Evaluating the influence of different correction sources (local base station and network-based).
- Analyzing positioning accuracy during semi-obstructed, open-sky, stationary and moving operation.
- Determining system limitations impacting precision landing performance.

This thesis will address these challenges through the design and experimental validation of an RTK (Real-Time Kinematic) enabled Unmanned Aerial Vehicle (UAV) positioning architecture that supports Precision Landing. This thesis was studied on the basis of operational needs in case of the RescueFly UAV hangar system [TUC3]. This provides both an evaluation context to assess the proposed positioning architecture and a target for integrating it into practice.

1.3 Research Objectives

The main goal of this thesis is to design and develop a GPS or more precisely RTK-based positioning framework for UAV precision landing applications by implementing and evaluating it. In order to achieve this main goal, Our specific objectives are defined as follows to make a comprehensive research of various GPS theory and equipment :

1. To study theoretical foundations of GNSS positioning techniques and RTK correction approaches and UAV navigation systems applicable to precision landings.
2. To combine multiple GNSS receiver modules with different hardware platforms (ZED-F9P, ZED F9R, Here+ RTK M8P) with a Pixhawk flight controller running ArduPilot software.
3. To configure and compare different correction sources such as a locally deployed RTK base station and the SAPOS network correction service.
4. To analyze interchangeability between different GNSS hardware platforms used as base and rover in order to analyze performance differences.
5. To design experimental settings for measuring accuracy of positions under static and dynamic test conditions both semi-obstructed and open-sky environments.

6. To analyze results from experiments and to characterize limitations of the system which affect reliability of centimeter level positioning.

7. To provide advice on how to improve precision landing performance and possible directions for future research including multi sensor fusion approaches.

1.4 Scope and Assumptions

The primary focus of this study was to evaluate the positioning accuracy of RTK GNSS-based precision landing applications for UAVs. This research focused on integrating hardware into an RTK GNSS system, evaluating correction configurations, and experimentally testing the system's performance. Development of new RTK algorithms were beyond the scope of this research effort. It was assumed that the Pixhawk flight controller with ArduPilot firmware would be used for operation of the UAV platform and that the GNSS receivers used in this study were commercially available, multi-frequency modules.

Considerations have been made regarding the assumptions associated with this research as follows:

- Use of standard configuration procedures for GNSS receivers by utilizing manufacturer provided tools (e.g., u-center).
- Communication links between the base station and rover remained stable throughout the course of experimental testing.
- RTK-fix conditions could be achieved in outdoor environments where there existed sufficient satellite visibility.
- Evaluation of precision landing accuracy for the UAV will be primarily based on positional measurement accuracy rather than full autonomous landing control algorithms.

Although the Here+ RTK M8P Rover was integrated and fix-status confirmed during our test, still quantitative accuracy measurements are outside the scope of study. Research topics including but not limited to; advanced vision-based landing systems, deep learning-based navigation algorithms, or full-scale autonomous mission optimization are outside the main scope of this work although they may represent areas for future extension.

1.5 Thesis Organization

This thesis contains ten chapters that are divided as follows: Chapter 1 Background, Motivation and Objectives of Research and Scope of Study. Chapter 2 Technical basis for GNSS Positioning, Error Sources and RTK Principles for UAV Applications. Chapter 3 State-of-the-Art Review of UAV Precision Landing, Identification of Gaps in Current Research Addressed in this Work.

Chapter 4 Description of System Architecture and Hardware Platforms for GNSS Used in Experiments. Chapter 5 Explanation of Correction Source Configurations (Local RTK

Base Stations and SAPOS Corrections Network). Chapter 6 Details of Software Configuration, Data Acquisition and Processing Framework Used for Experimental Evaluation.

Chapter 7 Description of Methodology for Experimentation, Test Environments, Measurement Procedures and Evaluation Metrics. Chapter 8 Presentation of Results from Experimental Performance Analysis of RTK-Based Positioning System. Chapter 9 Discussion on Observed Limitations and Practical Implications of the Findings. Finally, Chapter 10 Summarizes the Conclusions of our Research and Potential Directions for Future Work.

2 Technical Background

2.1 GNSS Fundamentals

GNSSs are called as space-based systems which enables global PNT capabilities; they include satellite constellations like GPS from US, Galileo (EU), GLONASS (RU), and BeiDou (CHN) [9], improving coverage, availability, and reliability, at the same time, they reduce dependency on individual systems in the use of multi-GNSS receivers [9].

2.1.1 GNSS Architecture

GNSS systems can be divided into three main components:

2.1.1.1 Space Segment Satellites orbiting around the earth which are mostly located in MEO at about 20,000 km altitude, and broadcasting navigation messages containing orbital parameters (ephemeris), clock corrections, and timing data for the receiving system.

2.1.1.2 Control Segment It helps to Monitor stations on the ground, record satellite orbits and clock performance, after that process the recorded data to produce corrected ephemerides and clock corrections, at last they are transmitted to satellites in order to maintain their positioning accuracy.

2.1.1.3 User Segment This component consists of GNSS receivers for collecting satellite signals, and determining its own position using trilateration, by taking advantage of signals from multiple constellations, it's task is to improve both accuracy and availability in difficult environments in places like urban canyons and mountainous [9].

2.1.2 GNSS Positioning Principles

GNSS positioning can be described as the measurement of signal delay times between satellites and receivers. Satellites broadcast timestamped signals that are synchronized to atomic clocks, and receivers measure the pseudorange which represents distance between receiver and satellite derived from the time which it took for the signal to propagate.

Using these typical pseudoranges measured from at least 4 satellites, the receiver will determine its 3-D position (latitude, longitude, altitude) and also its clock offset. The mathematical representation of this problem results in non-linear equations, and therefore the most common algorithms are used for solving this problem like least squares estimation or Kalman filtering.

The diagram shown in the figure 2 depicts the general GNSS positioning and augmentation process, as well as how a fixed or stationary reference base-station will provide corrections

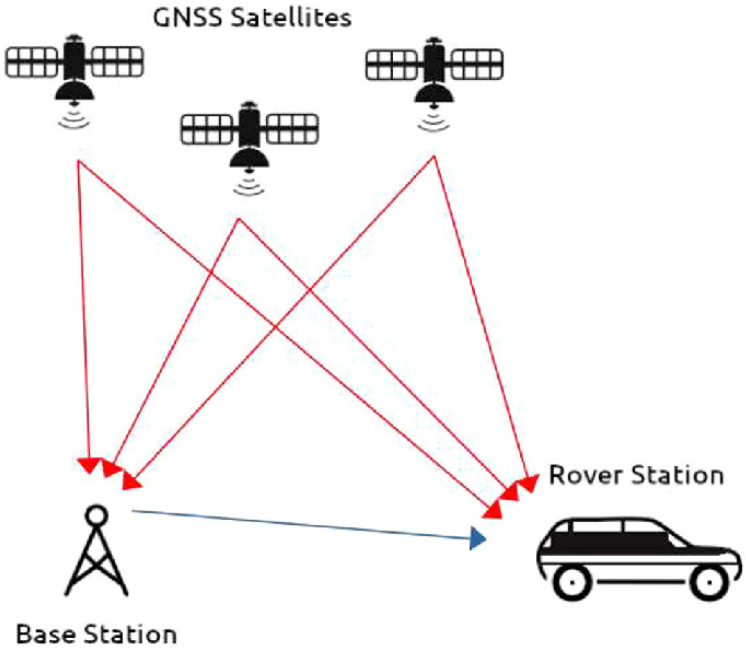

Figure 2: Conceptual overview of GNSS positioning [12].

to help the rover reduce common mode error through simultaneous observation of the same satellites.

Although standalone GNSS positioning provides an accuracy of about one meter, there exist many different error sources affecting this accuracy, like multipath reflections, atmospheric delays and satellite geometry, which can cause large errors [3]. Therefore, the integration of multiple constellations and the measurement of multiple frequencies can significantly decrease the uncertainties and increase the reliability of solutions [3].

2.1.3 Signal Structure and Measurement Type

GNSS satellites emit signals at multiple frequencies with ranging code and carrier wave. There exist two basic measurement types:

2.1.3.1 Code (Pseudorange) Measurements Provide meter level accuracy and are very commonly used for navigation.

2.1.3.2 Carrier Phase Measurements Provide millimeter level accuracy by tracking the phase of the carrier wave and need to be resolved with ambiguity resolving techniques for correct positioning.

Carrier phase measurements are the base of high accuracy positioning techniques like Differential GNSS (DGNSS) and Real Time Kinematics (RTK) positioning, which allow centimeter level accuracy if correction information is provided [6].

2.1.4 Multi-GNSS Integration

Multi-GNSS systems significantly improve satellite geometry and visibility, and thus availability in the case of obstructions. Multi-GNSS systems increase the number of observable satellites, reduce dilution of precision (DOP) and improve the reliability of positioning in dynamic scenarios like Unmanned Aerial Vehicle (UAV) navigation [10].

Recent studies have shown that integrating signals from multiple GNSS systems increases the redundancy and robustness against signal loss or interference, allowing for reliable navigation performance of autonomous aerial platforms [10]. Additionally, recent research has demonstrated that low-cost multi-frequency receivers exhibit significant improvement in terms of positioning performance compared to conventional single frequency receivers [9].

2.1.5 GNSS Accuracy

Standalone GNSS accuracy depends on the following factors:

- Satellite clock and orbit uncertainties
- Ionospheric and tropospheric delays
- Multipath propagation
- Receiver noise and hardware limitations
- Satellite geometry (Dilution of Precision)

In general, positioning errors caused by the lack of correction methods can reach several meters, and even more depending on environmental conditions [3]. As a result, modern precision navigation applications utilize augmentation methods such as Differential GNSS, Satellite Based Augmentation Systems (SBAS) and RTK GNSS to obtain a precision of centimeters.

2.1.6 GNSS in UAV Navigation

GNSS plays a crucial role in UAV navigation, providing autonomous flight control, waypoint navigation, georeferencing of images and precise landing capability. For all applications mentioned above, an accurate positioning is necessary.

Several recent studies have shown that GNSS-based positioning is still the primary means for global localization in UAV navigation, while sensor fusion with inertial sensors, cameras and LIDAR improve robustness in cases of signal blockage or interference [10]. Recent research has demonstrated that high-accuracy positioning technologies such as RTK GNSS are being integrated in UAV platforms to achieve the required precision of centimeters for autonomous landing and precision mapping applications [6].

2.2 GNSS Error Sources

Positioning accuracy in GNSS is impacted by numerous systematic and random error sources that derive from GNSS satellites, signal transmission, receiver hardware, and the environment. All of these error sources accumulate to generate the User Equivalent Range Error (UERE) that defines the achievable positioning accuracy in standalone GNSS systems. Observational quality assessments of recent GNSS receiver designs have indicated that measurement noise, multipath, blocked signals, and receiver hardware restrictions are all principal contributors to positioning uncertainty [9].

2.2.1 Satellite Clock and Ephemeris Errors

Errors associated with satellites are mostly due to inaccuracies in synchronization of atomic clocks on board the satellites and inaccuracies in orbital predictions of the satellites. Atomic clocks on board GNSS satellites are extremely stable, but there are always some residual drifts in the atomic clocks, and this causes a ranging error that is transferred directly to the positioning solution. Similar to the atomic clocks, satellite orbit prediction errors cause the calculated satellite positions used for trilateration to be inaccurate. This type of positioning error has a large effect on positioning accuracy when only broadcast ephemeris data is utilized [9].

2.2.2 Atmospheric Propagation Errors

Atmospheric delays in GNSS signal propagation represent one of the largest sources of GNSS positioning error because signals must travel through the ionosphere and troposphere before reaching the receiver. Changes in atmospheric conditions will change the speed of signal propagation and cause additional ranging delays that can exceed a few meters in magnitude if not properly modeled or corrected. Therefore, accurate modeling of the effects of the atmosphere is necessary to improve the positioning accuracy and reliability of both standalone and augmented GNSS systems [9]. Figure 3 shows how GNSS signal propagation is affected by ionospheric and tropospheric delays.

2.2.2.1 Ionospheric Delay The ionosphere is composed of charged particles that affect GNSS signals in a frequency-dependent manner to produce delays that depend on solar activity, location, and time of day. Single-frequency receivers are especially susceptible to ionospheric errors, whereas dual-frequency receivers can estimate ionospheric delays utilizing measurements from multiple frequencies. High accuracy positioning techniques such as RTK utilize differential corrections to minimize the impact of ionospheric errors [6].

2.2.2.2 Tropospheric Delay In addition to ionospheric delay, the troposphere produces additional signal delays due to changes in atmospheric gases, pressure, temperature, and humidity. In contrast to ionospheric delay, tropospheric delay is largely frequency independent and therefore can be modeled mathematically instead of compensating for it using multiple frequencies. Although residual tropospheric modeling errors can still affect centimeter-level positioning accuracy in high-precision GNSS applications such as RTK-based surveying and UAV navigation [5].

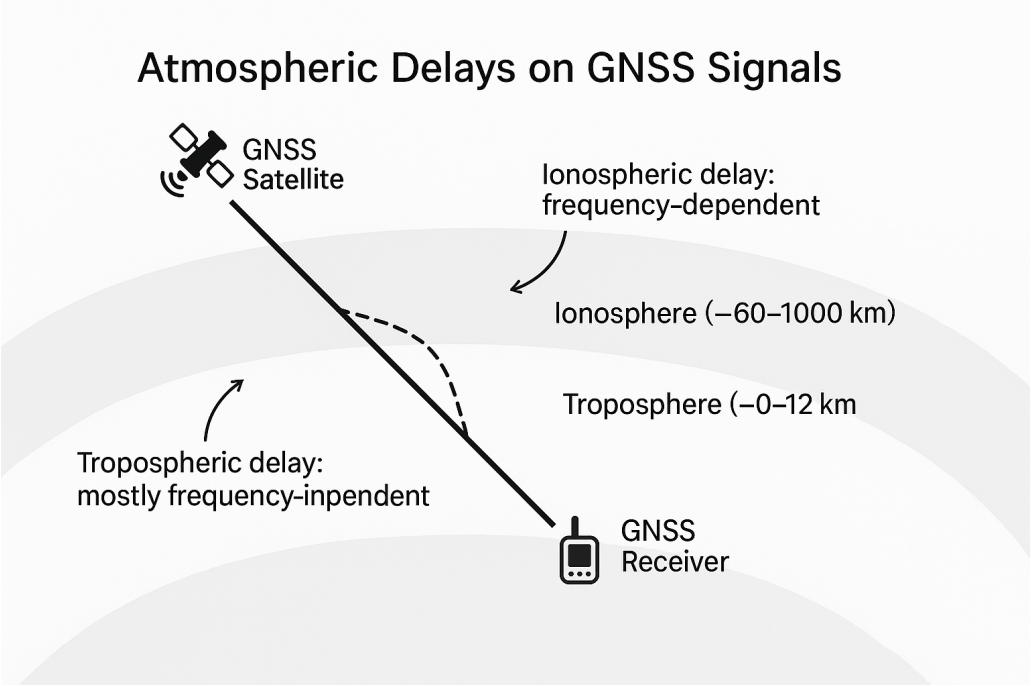

Figure 3: Conceptual illustration of ionospheric and tropospheric delays [48].

2.2.3 Multipath Errors

Multipath errors are produced when GNSS signals are reflected off surrounding objects such as buildings, terrain, or vehicles before being received by the receiver antenna. The reflected signals cause interference to the direct signal and distort pseudorange and carrier phase measurements, causing an incorrect position estimation. Experimental evaluations of UAV navigation systems indicate that multipath and signal obstruction degrade positioning performance and can severely degrade positioning performance in urban or partially obstructed environments [6].

2.2.4 Receiver Noise and Hardware Biases

Errors due to receiver hardware are generated by thermal noise, oscillator instabilities, antenna phase center variations, and hardware calibration imperfections, and influence positioning performance. Although errors due to receiver hardware are generally much smaller than errors due to the atmosphere and multipath, they do have a significant effect on positioning performance when positioning is constrained to centimeter-level accuracy [9].

2.2.5 Satellite Geometry and Dilution of Precision

Satellite geometry has an important role in determining how ranging errors are propagated into the final position solution. The geometric arrangement of visible satellites relative to the receiver is quantified using dilution of precision (DOP) metrics. Poor

satellite geometry, where satellites are clustered in a similar direction, amplifies the effect of measurement errors and leads to lower positioning accuracy. Multi-GNSS receivers provide improved satellite geometry by providing a greater number of observable satellites to decrease the value of DOP metrics and enhance the positioning reliability in dynamic applications such as UAV navigation [10].

2.2.6 Interference and Signal Blockage

GNSS signals are transmitted at extremely low power levels and therefore are highly susceptible to interference, signal attenuation or blockage, and intentional jamming. Obstacles such as buildings, vegetation, and terrain features can either attenuate or completely block GNSS signals and reduce the number of visible satellites and the positioning accuracy. Experiments involving UAV navigation systems demonstrated that environmental interference and signal obstruction can have a substantial effect on the positioning reliability of RTK positioning, highlighting the requirement for sensor fusion approaches that incorporate GNSS with inertial and vision-based systems [10].

2.3 Differential GNSS and Real-Time Kinematic (RTK)

Conventional standalone GNSS systems provide meter-level positioning accuracy due to satellite clock errors, atmospheric delays, multipath effects, and receiver measurement noise. Therefore, augmentation techniques like Differential GNSS (DGNSS) and Real-Time Kinematic (RTK) positioning have been developed to provide greater positioning accuracy than the traditional standalone system. These techniques utilize a network of reference stations to determine positioning corrections based upon their known locations, and then provide these corrections to the rover receivers to minimize the impact of common-mode errors and to enhance the overall robustness of the positioning solution. References include [6, 17, 24].

2.3.1 Principle of Differential GNSS (DGNSS)

Differential GNSS utilizes the concept that many of the primary sources of GNSS errors are correlated in space over relatively short distances. A reference station located at an accurately known position estimates range-domain errors by comparing the measured pseudoranges to the expected geometric ranges obtained from its known coordinates. The calculated correction terms are then transmitted to the rover, allowing it to improve the accuracy of the real time positioning solution [18].

At the rover, the corrected pseudorange can be represented as

$$\rho_{corr} = \rho_{meas} - \Delta\rho_{ref} \tag{1}$$

Where ρ_{meas} is the measured pseudorange at the rover and $\Delta\rho_{ref}$ is the correction determined at the reference station. In practice, differential corrections improve the accuracy of the positioning solution relative to a stand-alone GNSS solution, and this improvement is dependent on the distance of the rover from the reference station as well as the environment through which the rover is navigating [3, 18].

2.3.2 Reference Station and Rover Configuration

In general, a DGNSS/RTK positioning system consists of three primary components; (i) one or more reference stations that continuously operate and provide real-time corrections, (ii) a communication method to deliver the real-time corrections to the rover, and (iii) the rover itself which operates in a kinematic mode and combines the corrections provided with code and carrier phase observations to produce a high precision, real-time positioning solution. The longer the distance between the rover and the reference station, the weaker the spatial correlation of atmospheric errors becomes, and thus the less effective the differential correction will become. Network-based approaches, such as the creation of a Virtual Reference Station (VRS), allow the effective distance to be extended without loss of precision by utilizing multiple reference stations to model the regional error field [18, 19].

The Figure 4 represents the layout of a field-based stability experiment with at least one reference station and several rover stations located in the surrounding area in order to collect simultaneous GNSS/RTK data; the labeled rover stations demonstrate how the rovers positioning accuracy can be compared to the reference station in the same environmental conditions.

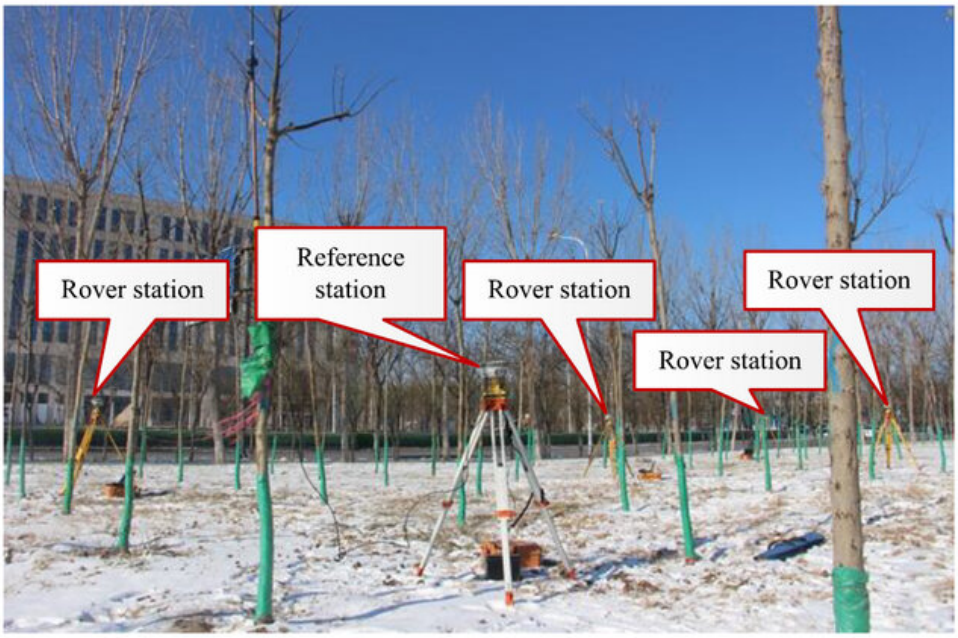

Figure 4: Experimental RTK setup showing the reference station and rover stations [25].

2.3.3 Carrier-Phase Based Positioning

While DGNSS primarily improves the accuracy of code-based (pseudorange) positioning, achieving centimeter-level accuracy requires the utilization of carrier-phase measurements. Carrier-phase measurements allow for highly accurate ranging, however they also introduce the integer ambiguity term that must be resolved. Research has shown that increasing the number of carrier-phase measurements from multiple GNSS constellations

increases the amount of redundancy available, and thus enhances the ability to resolve the ambiguity, especially in poor signal conditions [17, 24].

The carrier-phase observation equation is represented as follows:

$$\Phi = \rho + c(dt_r - dt_s) + I + T + \lambda N + \epsilon \tag{2}$$

Where ρ is the geometric range, dt_r and dt_s are the receiver and satellite clock offsets, I and T are the ionospheric and tropospheric delays, λ is the carrier wavelength, N is the integer ambiguity, and ϵ represents any residual noise or unmodeled effects.

2.3.4 Double-Difference Observation Model

Double-differences are utilized in RTK positioning to eliminate common satellite/receiver clock errors. Recent research on multi-GNSS RTK modeling has demonstrated that transitioning from a double-difference formulation to a single-difference formulation allows for increased flexibility while still providing strong ambiguity resolution performance when receiver-related biases are properly accounted for [17].

The double-difference carrier-phase model can be represented as follows:

$$\Delta\nabla\Phi = \Delta\nabla\rho + \lambda\Delta\nabla N + \Delta\nabla\epsilon \tag{3}$$

where $\Delta\nabla$ represents the double-difference operator.

2.3.5 Ambiguity Resolution and Initialization

RTK positioning typically begins as a *float* solution where the ambiguities are estimated as real values, and then transitions to a *fixed* solution once the correct integer value of each ambiguity has been validated. Research has shown that ambiguity biases, receiver-specific effects, and measurement noise can significantly degrade fix-rates, particularly with lower-quality sensors (e.g., smartphone-grade), and thus require robust ambiguity-validation strategies [20, 21].

Utilizing multi-frequency observations (e.g., L5/E5a/B2a) improve signal quality and strengthen the ambiguity model, thereby improving fix-rates and the accuracy of RTK positioning solutions versus legacy single-frequency processing. Results published in IEEE Internet of Things Journal demonstrate improved ambiguity fixing and positioning performance when utilizing modern signals and improved weighting strategies [24].

2.3.6 Real-Time Kinematic (RTK) Positioning

RTK positioning utilizes carrier-phase measurements along with real-time corrections delivered to the rover to achieve centimeter-level positioning accuracy. In practice, the rover combines code and carrier phase observations, applies corrections, determines state variables, and performs ambiguity fixing to produce a high-precision real-time positioning solution. Experiments involving multi-GNSS RTK positioning confirm that combining

multiple constellations improves the ambiguity-success-rate and the stability of the positioning solution, since additional satellites increase the strength of the model and decrease the sensitivity to outages [17].

The accuracy of RTK positioning typically reaches centimeter levels in open sky conditions, while the reliability of RTK positioning degrades in environments with multipath, obstructions, or signal interruptions. Reliability studies concerning UAV-related applications show that maintaining a fixed solution is dependent on signal conditions, antenna configuration, and the continuity of correction-links [6, 7].

2.3.7 Baseline Effects on RTK Accuracy

The performance of RTK positioning is heavily dependent on the length of the baseline between the rover and the reference station. Shorter baselines enable better cancellation of atmospheric errors, resulting in faster and more reliable ambiguity-fixing. As the distance of the baseline increases, ionospheric and tropospheric residuals increase and weaken the correction, which motivates the development of network RTK strategies such as VRS to preserve centimeter-level accuracy over larger areas [17, 18].

2.3.8 Network RTK and VRS Concept

Network RTK positioning employs multiple reference stations to estimate spatially-varying correction fields (such as ionospheric and tropospheric effects) and provide user-specific corrections. VRS methods synthesize a virtual base near the rover's location, allowing the rover to process data as if it were operating with a short baseline. Research presented in conference series on VRS technologies illustrates that multi-station networks improve the accuracy of medium and long-baseline positioning, and expand the area over which RTK services may be provided relative to those limited by the single-base RTK [18].

This Figure 5 compares traditional single-base RTK (in which a rover is receiving corrections from a reference station in close proximity), with Network RTK (such as VRS) in which many reference stations are used to create a modeled correction field. The image illustrates that Network RTK will typically allow for an operational area much larger than single-base RTK and provides greater spatial consistency.

2.3.9 Correction Transmission Protocols and Dissemination

Providing high-precision positioning requires the timely delivery of corrections. Network RTK dissemination research illustrates that correction-channel and bandwidth limitations directly affect achievable latency and solution continuity, which motivates the development of optimized dissemination strategies for high-accuracy navigation services [19]. Recent research published in IEEE Transactions on Instrumentation and Measurement has further investigated the delivery of RTK/PPP-RTK corrections via non-terrestrial networks, highlighting issues related to link capacity, correction rates, and practical convergence requirements for high-precision operation [23].

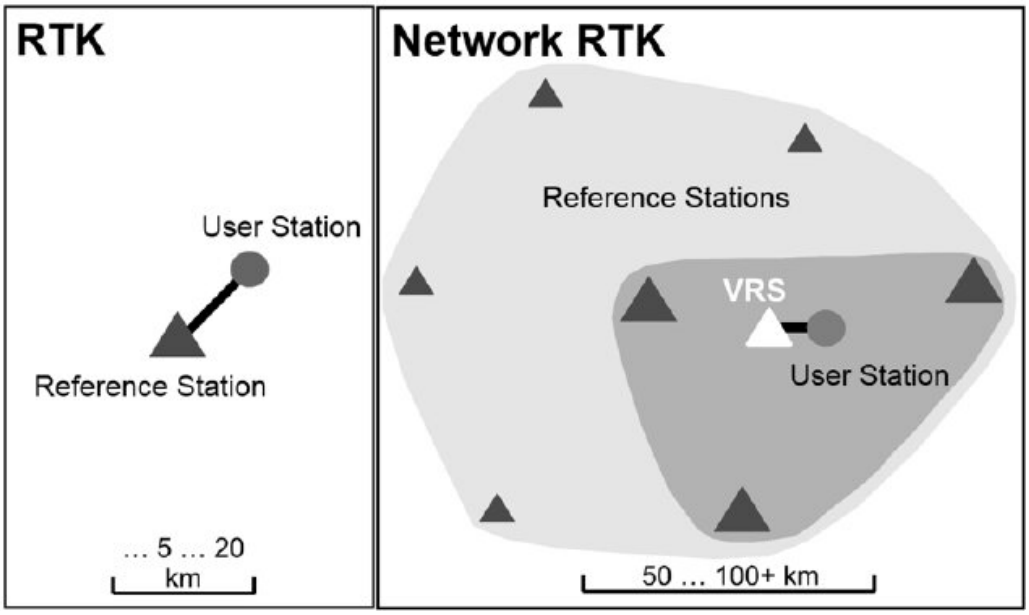

Figure 5: Architecture of a Network RTK system providing correction services to rover receivers [12].

2.3.10 Performance Comparison

Accuracy values in Table 1 are based on observed data quality, geometric relationships, baseline distance, and correction availability. Both multi-GNSS ambiguity resolution studies and UAV RTK reliability studies have shown that availability and fix continuity are equally important as nominal accuracy values for actual operational performance [6, 17].

Table 1: Typical Positioning Accuracy Comparison [3, 47]

Method	Horizontal Accuracy	Vertical Accuracy
Standalone GNSS	3–10 m	5–15 m
DGNSS	0.3–1 m	0.5–2 m
RTK	1–2 cm	2–5 cm

2.3.11 Advantages and Limitations of RTK

RTK provides high-precision positioning in real-time and is widely used in land surveying, robotics, and autonomous navigation. However, RTK positioning solutions can lose a fixed solution status due to multipath, obstructions, cycle-slips, or disruptions in the correction-link. Research investigating ambiguity fix behavior and real-time correction dissemination illustrate that robust ambiguity validation and continuous correction-delivery are critical for reliable RTK operation [19–21].

2.4 RTK for UAV Applications

The primary use of high-precision location data in various Unmanned Aerial Vehicle (UAV) applications (aerial surveys, photogrammetry, inspection of structures, autonomous navigation, precision landings) is achieved through the use of Real Time Kinematic (RTK) Global Navigation Satellite System (GNSS) technology. Although traditional GNSS systems provide meter level accuracy this is generally insufficient for the precision required for georeferencing in UAV based mapping, and autonomous landing procedures. The ability to provide centimeter level accuracy with RTK GNSS systems has greatly increased the effectiveness and dependability of UAV navigation systems [6, 7].

2.4.1 RTK-Enabled UAV Navigation

Many modern UAV platforms utilize RTK capable GNSS receivers to provide UAV flight control systems with the ability to accurately determine their location at any given time. RTK GNSS positioning enhances the accuracy of waypoints in UAV navigation systems, increases the accuracy of navigation systems while hovering, and improves the overall reliability of navigation systems in UAV autonomous missions. Several studies have evaluated UAV navigation system performance using RTK GNSS positioning and found that when compared to the use of GNSS alone, RTK GNSS positioning provides substantial reductions in horizontal and vertical positioning errors. Therefore, UAVs are able to fly along predetermined paths with much greater accuracy [7].

In addition to improving the accuracy of UAV navigation systems, RTK GNSS positioning also improves the reliability of sensor fusion algorithms used to combine GNSS data from an IMU. Since the positioning provided by the RTK GNSS system is highly accurate it greatly reduces the amount of error associated with the accumulated inertial drift, and therefore improves the stability of UAV state estimation, especially during long duration flights and/or UAV autonomous missions [10].

2.4.2 Precision Landing and Autonomous Operations

RTK GNSS is a crucial component of the systems utilized to enable precision landing capabilities for UAVs. The accurate positioning information provided by RTK GNSS enables autonomous landing systems to guide UAVs to a predefined landing location with centimeter level precision, which is necessary for applications such as automated charging stations, logistics delivery platforms, maritime UAV operations, etc. The necessity for high precision localization is even more evident for landing on moving or confined platforms since even small positioning errors can result in mission failure [4].

Additionally, RTK GNSS positioning enhances the safety of autonomous UAV operations by enabling precise geofencing and reliable position monitoring. The ability to obtain centimeter level positioning information in real time enables flight control systems to strictly adhere to operational boundaries, thereby reducing the risk of navigation errors and increasing the overall safety of autonomous UAV missions [6].

2.4.3 System Design Considerations for UAV RTK Integration

There are several factors affecting the performance of RTK GNSS positioning in UAV applications. Some of the most common factors include the placement of the antenna, signal obstruction, multipath errors and communication latency between the reference station and the UAV GNSS receiver. Research on UAV antenna configuration design and installation has shown that improved antenna designs and installation techniques can significantly decrease multipath errors and increase the RTK GNSS positioning stability during flight [5].

Also, it is very important for UAV RTK systems to have continuous access to reliable correction transmissions, because communication disruptions can make the RTK GNSS positioning solution go back to floating mode or standalone GNSS accuracy levels, emphasizing the importance of robust communication infrastructure for UAV RTK systems operation [6].

2.4.4 Future Trends in UAV RTK Positioning

The recent development of multi-constellation and multi-frequency GNSS receivers has further improved the reliability of RTK GNSS positioning in dynamic environments. Network RTK services, and real-time corrections delivered through cellular communication networks are now enabling high-precision positioning over larger geographic areas than before possible without the need for local base stations. These technological advancements will likely play a major role in the implementation of autonomous UAV systems for urban air mobility, automated inspection and large scale mapping operations [7].

3 State of the Art and Research Gap

3.1 Precision Landing Methods

Precision landing is one of the most important elements of autonomous UAV mission execution, as the UAV must be able to safely and accurately land on designated landing pads, such as charging pads, docking stations, rooftops or other mobile platforms. Landing accuracy and robustness are critical, as errors that would be acceptable during flight can be hazardous during the final descent. Surveys and analysis of UAV systems have indicated that the landing phase of autonomous UAV operation is currently the most difficult phase of UAV operation due to the stringent accuracy, reliability and environmentally robust requirements for landing [1]. As a result, the area of precision landing has become an active area of research with several prominent families of methods: GNSS based landing (primarily RTK/NRTK), vision based landing, beacon assisted landing and multi-sensor fusion architectures.

3.1.1 GNSS Based Precision Landing Methods

Methods of GNSS-based precision landing utilize satellite signals to determine the position of a UAV. Stand-alone GNSS typically produces positioning accuracies of meters, which is inadequate for precision landing and repetitive docking tasks [3, 16]. Real Time Kinematic (RTK) techniques employ carrier phase measurement with differential corrections provided from a reference station (base) or a correction network (Network RTK) to achieve positioning accuracies in the order of centimeters [13, 17].

3.1.1.1 Local Base Station RTK (Base-Rover) Landing A popular way to implement a local base station RTK landing setup is to deploy a base station near the landing zone and have it continuously broadcast RTCM corrections to the UAV's receiver. Local base-rover setups can produce very good precision and repeatability when operating in a favorable environment, and are commonly used in research prototypes and controlled demonstrations. Both the performance and feasibility of RTK based navigation and landing have been demonstrated experimentally in various landing/localization scenarios, including those requiring precise localization near a target or platform [4]. However, local base-rover setups require careful configuration and stable communication links to maintain performance and can degrade under certain circumstances, including loss of correction delivery and loss of satellite visibility.

3.1.1.2 Network RTK (NRTK), VRS and correction services Instead of utilizing a physical base station, network RTK employs a network of reference stations to model spatial errors and provide corrections (e.g., VRS). The RTK network concept and its evolution are described in classic network RTK works, including reference-station network-based RTK system concepts and implementation perspectives [14, 15]. VRS related correction strategies are also examined in more recent work focusing on correction information and virtual reference station techniques [18]. Network RTK is appealing for operational UAV deployments since it eliminates the requirement for local infrastructure and can provide

corrections across a wide geographic region. On the other hand, constraints imposed by correction dissemination (latency, bandwidth, and communication reliability) can negatively affect positioning performance, especially for mobile platforms like UAVs [19].

3.1.1.3 Accuracy and reliability constraints (UAV specific)

Even though RTK can provide centimeter level positioning accuracy, there are numerous factors that affect the actual landing performance in real world applications. These factors include the location of the antennas and the design of the ground plane, the quality of the receiver, the presence of multipath conditions, and the stability of the corrections. Studies focused on UAV specific RTK demonstrate that the placement of the antennas (i.e., adding ground planes) affects the quality of RTK positioning, which directly relates to landing repeatability [5]. In addition, low cost receiver studies show that the hardware and software of the receiver affects the quality of the observations and the resulting positioning outcome [9]. Reliability focused studies on UAV RTK demonstrate that both environmental conditions (multipath, partial obstruction) and operational conditions (loss of correction link) can result in solutions that fail (float or standalone), which can result in uncontrolled position jumps during the final descent [6]. Recent analyses of RTK positioning behavior for UAV applications highlight that RTK performance varies depending on the dynamic conditions and operational context of the UAV, thus supporting the need for systematic testing instead of assuming perfect centimeter accuracy at all times [7].

3.1.1.4 Relevance of Multi-GNSS and Ambiguity Resolution to Landing

Ambiguity resolution is necessary for achieving the desired accuracy for RTK positioning. Failure to resolve ambiguities correctly and/or rapidly results in lower accuracy positioning. There are numerous well-established ambiguity resolution algorithms (e.g., LAMBDA) that are utilized in RTK processing pipelines [13]. Recent work in multi-GNSS RTK ambiguity resolution (including methodological shifts from double-difference to single-difference handling) demonstrates that improved processing capabilities enable faster and more robust ambiguity resolution [17]. While the previous studies were not UAV specific, the underlying theme applies directly to UAV landing applications: better ambiguity resolution and use of multi-GNSS tends to increase the likelihood of maintaining an RTK fix solution, which is necessary to maintain consistent landing accuracy. Correction delivery research is also relevant: constrained communication links can negatively affect the quality of corrections, motivating research in low bandwidth correction dissemination and alternative correction delivery channels [19, 23]. For UAV operations that rely on mobile networks, such constraints may be observed during field operations, especially at low altitudes where connectivity may fluctuate.

3.1.2 Vision-Based Precision Landing Methods

Vision-based precision landing methods compute the relative position of the UAV using onboard cameras. A typical vision-based landing workflow includes detecting a fiducial tag or a learned target and computing the relative position for the final approach. Deep learning has become increasingly popular in target detection, for example, YOLO-based detection has been used to support high-precision landing on a moving platform using vision-based guidance [11]. Vision-based landing methods are particularly attractive close

to the ground since they can provide relative accuracy that exceeds GNSS in challenging GNSS reception conditions.

However, vision-based landing methods are sensitive to lighting and visibility conditions, motion blur, camera calibration, and occlusions. Furthermore, many vision methods require significant computational resources and robust pipelines to perform in real time. Therefore, vision is frequently combined with GNSS/INS instead of being used independently, especially when the UAV must travel long distances between waypoints and only use vision in the vicinity of the landing zone. In practical systems, vision can be viewed as a terminal guidance sensor that enhances the landing alignment after the GNSS/RTK has positioned the vehicle in the vicinity of the landing target [2, 10].

3.1.3 Beacon Assisted Precision Landing Methods

Beacon-assisted precision landing methods utilize installed infrastructure at the landing site to provide the UAV with relative positioning data. Commonly used technologies include ultra-wideband (UWB), infrared beacons, and radio frequency (RF) transmitters. UWB positioning is generally considered to be robust in constrained or semi-obstructed environments since it can provide accurate ranging and localization, often with decimeter level (or better) accuracy dependent upon the configuration. A study focused on UWB positioning systems specifically emphasizes the suitability of UWB-based positioning systems in harsh environments and the trade-off between infrastructure and robustness [12].

For UAV precision landing, beacon-based systems can provide reliable and consistent relative positioning in the vicinity of the landing pad, allowing for reliable docking behavior even under GNSS degradation. The major disadvantage of beacon-based systems is their lack of scalability; beacon-based systems require the installation of infrastructure at every landing site, thus limiting their applicability to wide-area operations unless the landing sites are fixed and controlled (e.g., warehouses, industrial campuses, charging networks).

3.1.4 Multi-Sensor Fusion Precision Landing

The current state-of-the-art for UAV precision landing methods is multi-sensor fusion, which combines the outputs of complementary sensors to enhance the robustness of the system. Sensor fusion can be loosely coupled (combining independent solutions) or tightly coupled (combining raw sensor measurements into a single estimator). A typical architecture for UAV landing utilizes GNSS/RTK for global positioning, IMU for predicting motion at high rates, and either vision (or LiDAR/UWB) for accurate relative positioning during the terminal phase. Using multiple GNSS receivers to create a multi-GNSS receiver configuration and integrating the outputs of these receivers can further enhance the robustness of the system by increasing the number of satellites available for positioning and improving the geometric diversity of the constellation. Research on estimating the position and orientation of a UAV using multiple GNSS receivers supports the notion that redundancy in the number of antennas/receivers can increase the reliability of navigation and orientation determination [2]. Testbeds focused on multi-modal UAV navigation have shown that fusing the outputs of multiple sensing modalities enables reliable navigation in environments where GNSS is unreliable [10]. Thus, for landing applications, if RTK

temporarily fails (e.g., float solution), the UAV can continue to maintain a stable estimate of its state using inertial propagation and local sensors until high precision measurements are again available.

3.1.5 Comparative Analysis and Practical Selection Criteria

Each family of landing methods offers advantages and disadvantages for deployment:

- **RTK/NRTK GNSS landing:** provides globally scalable and infrastructure light (especially NRTK) with centimeter level accuracy in favorable conditions; however, is affected by multipath, partial obstruction, correction latency and availability of corrections [6, 7, 19].
- **Vision-based landing:** provides excellent relative accuracy in short range and supports landing on moving/marked targets; however, performance is affected by environmental visibility and computational stability [11].
- **Beacon-assisted landing (e.g., UWB):** provides extremely reliable relative positioning in controlled areas; however, requires installation of infrastructure at each landing site, thus limiting scalability [12].
- **Multi-sensor fusion:** provides the best overall robustness and continuity; however, increases system complexity and calibration requirements but provides fault tolerance to single sensor failures [2, 10].

In practice, hybrid systems are becoming increasingly prevalent: RTK GNSS is utilized as the primary global positioning source and either vision or beacons are employed to enhance the accuracy of the terminal phase and provide redundancy under GNSS degradation. This hybrid view point aligns with current UAV research trends that emphasize the development of robust UAV navigation architectures versus individual sensor solutions [1, 10]. For the purposes of this dissertation (evaluation of RTK enabled UAV positioning for landing), the performance of RTK under various hardware configurations, correction sources and environments represents a critical basis for evaluating whether additional sensors are needed and where system limitations exist [5–7, 9].

3.2 Review of Existing Research

High-precision uav positioning and landing research has advanced in recent years through advances in both real-time correction infrastructures for GNSS technologies and ambiguity resolution algorithms with multi-sensor navigation frameworks. Over the last two decades the combination of these developments have allowed for centimeter level positioning performance to be achieved in mobile platforms such as UAVs. This section discusses key research contributions in the area of RTK positioning theory and its application to uav positioning performance evaluation; development of correction networks; and multi-sensor navigation approaches relating to precision landing applications.

3.2.1 Advances in High-Precision GNSS Positioning Theory

Modern carrier phase differential GNSS navigation systems are built on differential positioning concepts. The LAMBDA method was one of several efficient ambiguity resolution techniques introduced to enable the reliable real-time estimation of integer ambiguities and improve RTK positioning convergence performance [13] and these foundational methods still serve as a key component of many RTK processing chains currently utilized by UAV navigation systems.

Following this, researchers continued to develop new ambiguity resolution techniques that could be applied to multiple GNSS constellations. A number of multi-GNSS RTK positioning methods have been developed that utilize data from multiple satellite constellations to improve satellite visibility, to create stronger observation geometry, and to add redundancy to the measurement process. In addition to improving ambiguity resolution success rates and reducing ambiguity resolution convergence times, multi-GNSS processing provides increased positioning reliability under partially obstructed observational conditions [17]. Other studies have examined the effects of various factors on positioning performance in realistic receiver environments including the quality of observations, signal tracking stability, and stochastic modeling [20, 21], particularly with low-cost and/or smartphone grade GNSS receivers. Recent studies have demonstrated that multipath interference, signal attenuation, and environmental obstructions can reduce the reliability of ambiguity resolution, prompting further research into robust ambiguity estimation techniques that will maintain positioning performance during adverse operating conditions [22].

The recent development of additional GNSS frequency bands and modern multi-frequency signals has also provided researchers with the opportunity to explore the potential benefits of utilizing these types of signals. The utilization of multi-frequency signals increases the ability to mitigate errors caused by the ionosphere and allows for faster ambiguity resolution, thereby increasing RTK positioning availability and accuracy in dynamic navigation applications [24]. These developments provide the theoretical and algorithmic foundations for modern high-accuracy UAV navigation systems.

3.2.2 Correction Infrastructure and Network RTK Developments

Beyond algorithms for positioning, correction infrastructure is also key to making practical RTK navigation systems possible. Earlier RTK positioning depended on single-base reference stations transmitting differential corrective data to rover receivers within a limited operational range. While effective in localized applications, single-base RTK systems have a reduced performance over longer baseline distances due to spatially varying atmospheric errors and other satellite-related errors. In order to address these limitations Network RTK architectures were developed which combine measurements from multiple reference stations to generate regional correction models and virtual reference station (VRS) solutions [14, 15].

The use of interpolating atmospheric and satellite related errors through VRS techniques has been demonstrated to significantly improve the accuracy of positions determined by Network RTK methods and reduce the growth rate of error with respect to baseline length for mobile users such as UAV platforms [18]. Furthermore, the performance of

Network-based correction services relies strongly on the reliability and latency of communication links that deliver correction messages. Studies examining dissemination methods of corrections highlight the importance of low latency data transmission and bandwidth efficient correction encoding to maintain continuous RTK-fix positioning solutions in dynamic navigation environments [19].

More recent work has examined the feasibility of providing high-precision GNSS corrections via non-terra-stationary Network (NTN) plans such as satellite communication systems. Preliminary studies indicate that NTN-based correction delivery could enable high-precision positioning service in remote or infrastructure-limited regions and therefore extend the operational coverage of RTK positioning technologies [23]. These developments suggest that correction delivery mechanisms will continue to evolve alongside positioning algorithms in order to support large scale UAV navigation applications in the future.

3.2.3 Experimental Evaluation of RTK GNSS in UAV Applications

A growing body of research evaluates the use of real time kinematics (RTK) positioning technologies in Unmanned Aerial Vehicle (UAV) applications. Photogrammetry based research indicates that the improvements in positioning accuracy of one centimeter or better that result from using RTK corrections and Network RTK corrections in UAV mapping applications improves UAV mapping accuracy as well as improves UAV georeferencing accuracy as compared to non-RTK corrected data. Further, research indicates that RTK corrected data can significantly reduce the number of Ground Control Points (GCPs) needed for UAV mapping and survey applications, thus improving survey efficiency [3].

Reliability-based studies of UAV RTK positioning performance show that there are many environmental conditions (i.e., satellite line-of-sight, multipath interference, etc.) that have a significant effect on the achievable positioning accuracy in UAV RTK positioning [6] [7]. In dynamic UAV flight, interruptions of RTK corrections and/or poor observation quality during RTK corrections can result in temporary floating solutions or unstable positioning during UAV operation; therefore, reliable communications and observation conditions are necessary for UAV operation.

Research into the design of antenna ground planes and antenna mounting configurations have shown that there are significant differences in positioning accuracy of UAV when the antenna's electromagnetic (EM) characteristics are optimized for the UAV's installation environment [5]. Likewise, research into low-cost Global Navigation Satellite Systems (GNSS) receivers indicate that the receiver's ability to track signals, the type of signal processing algorithms utilized by the receiver, and the amount of noise present in the receiver's measurements all impact the stability of the positioning system and the achievable positioning accuracy of the system [9]. The implications of these results indicate that it is extremely important to carefully select and configure both the hardware and receive components of a UAV positioning system to ensure the desired positioning accuracy for UAV applications such as high precision landing operations.

3.2.4 Multi-Sensor Navigation and Fusion Approaches

The development of multi-sensor integration technology is a critical component of improving the reliability of UAV navigation systems. Through the use of multi-GNSS receivers

and redundant positioning architectures, researchers have shown that measurement redundancy increases and it is possible to estimate the attitude of a UAV with multiple antennas [2]. Researchers have developed multi-modal UAV navigation testbeds utilizing GNSS, inertial sensors, and other sensing modalities that show the ability to develop stable UAV navigation solutions using sensor fusion techniques even when GNSS signals are temporarily unavailable [10].

Researchers have also shown significant interest in developing vision-based landing guidance systems for UAVs. For example, researchers have developed deep learning-based object detection systems for landing target detection (e.g., YOLO) that have shown promising results in detecting landing pads and determining the relative position of the UAV during the final approach/landing phases [11]. These types of systems are useful in UAV operations where GNSS positioning accuracy is reduced due to signal blockage or multipath interference. However, because they depend on visual conditions of the environment, they do not make good stand-alone UAV navigation solutions; therefore, researchers are working to integrate them into existing GNSS-based positioning frameworks.

Infrastructure-assisted positioning technologies such as ultra-wideband (UWB) localization systems provide another means for achieving high precision relative positioning within controlled environments. Research has shown that UWB positioning systems can provide high positioning accuracy in infrastructure supported environments; thus, they are a good candidate for docked or industrial landing applications [12]. However, the need for infrastructure restricts the potential for widespread application of UWB positioning systems for UAV navigation in uncontrolled environments.

3.2.5 Related Research at TU Chemnitz

TU Chemnitz researchers under Professorship of Computer Engineering at Chemnitz University of Technology has produced a body of work defining the operational context for this thesis. These contributions have addressed autonomous UAV infrastructure, cloud-based mission coordination, real time monitoring, UAV based inspection and collectively defined the system boundaries in which a precision landing solution can be expected to function.

Battseren et al. [TUC1] demonstrated when using GPS grade geolocation techniques an average position error of 4.59 m is achieved, a result that clearly motivates the use of RTK level correction data when attempting to achieve centimeter level landing accuracy.

Bayasgalan et al. [TUC2] documented structured UAV inspection campaigns across 78 power line towers, documenting the flight protocols and methodologies used to empirically validate the performance of UAVs, methods that are similarly relevant to evaluating the performance of landing maneuvers.

Harradi et al. [TUC3] provide a decentralized UAV hangar for water rescue missions using a 1.76 m x 1.76 m landing pad, ArUco marker guidance and a mechanical repositioning module that will move the UAV after landing so it will touch down in alignment with the charging contacts. The required repositioning indicates that the 0.15 m landing accuracy that was achieved does not satisfy the requirement to land on the charging contacts without mechanical assistance.

Harradi et al. [TUC4] expand upon this by providing a cloud-based MAVLink architecture that governs all aspects of the mission from preflight planning to post-flight analysis, using a custom command dialect that includes a specific clearance command `MAV_CMD_RF_LANDING_CLEAR`. The authors do not describe either the UAV side descent state machine or how mid-descent failures are handled.

Kilic et al. [TUC5] have developed a WebRTC-based multi-UAV ground control station that achieves 85 – 120 ms transmission latency, and point out that GPS, IMU and compass sensors can fail to function when in close proximity to high voltage electrical equipment due to electromagnetic interference.

Tudevdagva et al. [TUC6] proposed a conditional autonomy model for inspecting High Voltage Transmission Lines (HVTL), requiring a continuous readiness assessment of all available sensors before continuing the mission, a principle that is also relevant to the design of RTK landing systems.

Across all six contributions, there is no specification of a precision landing controller, there is no description of how to monitor the quality of the RTK solution as a precondition to authorizing the descent phase of the mission, and there is no description of how to define a UAV side state machine to coordinate the execution of the descent sequence with the clearance protocol of the hangar. This void is the primary operational basis for this research thesis.

3.3 Research Gap Analysis

Although there has been great advancement in GNSS positioning technology, RTK correction infrastructure and UAV based navigation systems [13], many major issues still exist regarding the implementation of UAV precision landings. The existing literature demonstrates several experimental and technological issues that support the need for the research outlined within this thesis.

3.3.1 Limited Comparative Evaluation of GNSS Hardware Platforms

The majority of the literature examining RTK enabled UAV position systems (using GNSS) are limited to a single receiver platform or a single antenna configuration. Therefore, it is difficult to make generalization to other hardware configurations from these studies. Studies of antenna design and receiver characteristics demonstrate that positioning performance is directly affected by hardware configuration, quality of observations and performance of signal tracking [5, 9]. Despite the importance of understanding how hardware configuration impacts positioning performance, there remains a lack of systematic comparative studies using multiple commercial multi-frequency GNSS receivers operating under the same conditions.

With the rapidly emerging availability of low cost multi-frequency GNSS modules capable of RTK positioning, there exists an immediate need for comprehensive experimental testing of various hardware platforms to assess performance differences, interoperability and applicability to precision landing missions. These performance differences are especially relevant for UAV operations due to payload limitations, power consumption, and communication interfaces which all impact the choice of hardware.

3.3.2 Insufficient Comparison of Correction Infrastructure Performance

Another shortcoming noted by prior research was that there were no comprehensive experiments comparing RTK corrections through a variety of methods. The two most common correction methods; single base RTK and Network RTK have been in use for years but very few studies have compared the two systems in terms of performance in terms of cost. Most comparative experiments compare a single correction method which does not allow for evaluation of the performance trade offs when using local base stations versus using a network based service. Studies on Network RTK architectures and VRS show that regional correction models can provide greater accuracy than other correction models with better scalability [14, 18]. On the other hand, studies on correction dissemination highlight the critical role that reliable communication and low latency play in maintaining an RTK-fix solution [19].

As such, studies that experimentally compare correction performance among various RTK correction methods in the context of UAV positionning remain relatively rare. These types of studies will be especially important in the development of future UAV applications where communication conditions will vary greatly from place to place and/or where both local base stations and national correction networks will be available as potential correction alternatives.

3.3.3 Limited Evaluation Under Diverse Operational Environments

Many field tests of RTK UAV positioning have been performed in open-sky test beds which are ideal environments for satellite signals to be visible to all satellites and communication conditions to be stable. The results from these tests show that RTK systems can provide a very high level of positional accuracy but the results of these tests were in controlled conditions. The controlled conditions of these tests do not reflect the realities of real-world operation and there are many ways in which the positioning performance of RTK systems can be degraded by the environment in which it operates; e.g., signal blockage, multipath, etc [6, 7].

There has been relatively little systematic testing of RTK enabled UAV positioning systems across multiple operational scenarios (semi-obstructed, open-sky, static, dynamic) to assess the impact on positioning accuracy and availability of corrections, as well as landing reliability. Dynamic flight tests, specifically those including trajectory motion and maneuvering, are critical to assessing the stability of the system's ability to navigate during the actual landing phase.

3.3.4 Integration Challenges Between Navigation Components

There is another gap in GNSS receiver, flight controller and correction communication pipeline integration into operational UAV systems. Although many studies look at a single positioning algorithm or sensor fusion method, few studies have provided an evaluation of the practical challenges associated with integrating the entire system (hardware compatibility; data interface configurations; synchronizing all of the navigation subsystems) and the development of multi-modal UAV navigation testbeds demonstrates the potential benefits of an integrated sensor architecture [10] but there are very few experimental

studies assessing the reliability of and developing configuration strategies for integrating RTK-enabled UAV platforms.

It is crucial to address these integration challenges so that the precise positioning performance that is often achieved in controlled laboratory environments can be consistently replicated in real world UAV deployments. For example, it is important to assess how various communications interfaces, firmware configurations and correction data processing affect positioning performance.

3.3.5 Baseline Evaluation Prior to Advanced Sensor Fusion

The development of multisensory fusion methods (combining GNSS, Inertial Sensors, Vision Systems and Infrastructure Assisted Positioning) will significantly enhance UAV navigation reliability [2, 11]. However, prior to the evaluation of multisensory fusion methods in terms of their contributions to improved landing accuracy, there are still fundamental limitations that need to be understood with respect to standalone RTK GNSS based positioning systems. Establishing an appropriate RTK GNSS positioning baseline, enables researchers to quantitatively evaluate the contributions of multisensory fusion methods towards enhanced UAV landing accuracy.

3.3.6 Absence of Precision Landing Integration in Existing UAV Hangar Systems

The UAV autonomous deployment systems discussed in Section 3.2.5, represent a fully functional deployment system; however, there is no component within these systems that specifically addresses the precision landing problem at the navigation level. For example, the RescueFly hangar [TUC3] is able to achieve only 0.15 m of landing accuracy which is then corrected by the mechanical re-positioning of the aircraft after landing, as opposed to having the precision at the navigation level during the landing process. Additionally, the MAVLink coordination architecture [TUC2] defines the `MAV_CMD_RF_LANDING_CLEAR` clearance command, but does not specify the UAV side logic for the descent process (i.e., RTK solution quality verification, multi-phase approach sequencing, and abort handling). Furthermore, the real-time monitoring system [TUC1] provides the communication channel to observe telemetry data, but does not include monitoring/assessment of landing state or positioning quality. Finally, the conditional autonomy model proposed for HVTL inspection [TUC6] illustrates that sensor readiness should be the gatekeeper of the mission progress, but this principle has not been applied to the landing portion of any TUC system. Lastly, the geo-localization pipeline [TUC4] demonstrates that standard GPS positioning yields average positioning error of 4.59 m, which is an order of magnitude larger than what is required for precision landing. Therefore, it can be concluded that standard GNSS will not be sufficient for this particular application.

This gap is different in nature than the other five gaps described in Sections 3.3.1-3.3.6. While the previous gaps address issues within the positioning literature, this gap refers to the lack of an operational UAV landing system. This gap directly affects the current design of the UAV and thus the UAV's ability to perform missions without compromising safety and/or performance. The primary focus of this thesis is addressing this gap by developing, implementing, and experimental validation of an RTK-enabled positioning

architecture that will integrate with the existing RescueFly hangar system and provide the previously unspecified UAV-side landing logic.

3.3.7 Research Contributions of This Thesis

This thesis provides a comprehensive experimental study of RTK enabled UAV positioning systems and addresses the identified gaps as follows:

- A comparative assessment of several different multi-frequency GNSS receiver systems that are capable of being used interchangeably as a rover or base station.
- A laboratory study comparing the performance of an RTK base station operating from a local reference point with corrections provided by a service provider over a network for the same measurement conditions.
- A systematic evaluation of the performance of the entire system using static and dynamic measurements made semi-obstructed and open-sky conditions to examine how the environment influences positioning accuracy.
- An examination of how the components of a system integrate together including the configuration of the receivers, the integration of the flight controller into the overall system, and the reliability of the communication of correction data.

By examining the above challenges the proposed experimental design will aid in an enhanced comprehension of practical application considerations for RTK-based UAV precision landing systems; and provide a basis for future study of the integration of multi-sensor landing architecture.

4 System Architecture and Hardware Description

4.1 Overall System Architecture

This thesis has established an overall system architecture to enable precise UAV positioning, and precise landing through the use of high-precision RTK-GNSS technology. The architecture provides a modular integration of GNSS receiver systems that provide a rover–base configuration, a flight control unit, communication links to transmit corrections to each rover and all necessary ground-based systems for generating corrections and monitoring rover performance. Modular RTK-enabled UAV navigation architectures are well represented in the literature on recent UAV positioning studies and testbeds for multi-sensor UAV navigation [2, 10].

4.1.1 System Design Principles

The design of this system was guided by three main goals: modularity, compatibility and experimental flexibility. This modular system design allows for individual assessment of each of the GNSS hardware modules, correction systems and flight control module integration. Compatibility will enable all types of GNSS receivers to be utilized as both a base and a rover unit without loss of function in operation. Experimental flexibility will allow for the development of an organized test methodology to evaluate the system's performance while utilizing multiple types of correction infrastructure, such as local RTK base stations and national reference station networks for network-based correction services.

The system utilizes the standard RTK navigation architecture model where there is a base station providing corrections to a rover receiver installed on the UAV. Carrier phase observations from the base station are sent to the rover through communications links as RTCM correction messages. The rover uses the corrections provided along with the satellite observations in real time to develop centimeter level position estimates and provide them to the flight controller to utilize for navigation and landing purposes [14, 17].

How all major hardware and software components are interconnected to each other, figure 6 shows a complete image of the system architecture which was studied during this thesis. According to this diagram, RTCM corrections are sent using either Radio, NTRIP or TCP-IP protocol to the rover. The GNSS receiver is mounted on the rover to apply RTK correction after receiving the correction from the base station to achieve a centimeter level of accuracy.

4.1.2 Base Station Segment

The base station segment - a base station is equipped with a fixed GNSS receiver installed at a surveys reference location. The primary function of the base station is to compute differential corrections by comparing measured satellite signals to known reference coordinates. These corrections account for satellite clock errors, atmospheric delays and other systematic measurement errors that affect the positioning accuracy of the rover. There has been extensive research on reference station Network architectures and their

error modeling capabilities in Network RTK literature [14, 15]. This work implemented a local base-station configuration where the base receiver continuously transmits RTCM correction data to the rover via telemetry communication channel. In addition, this work supports external correction sources such as national RTK services; therefore it allows comparative evaluation between locally generated and Network provided correction streams.

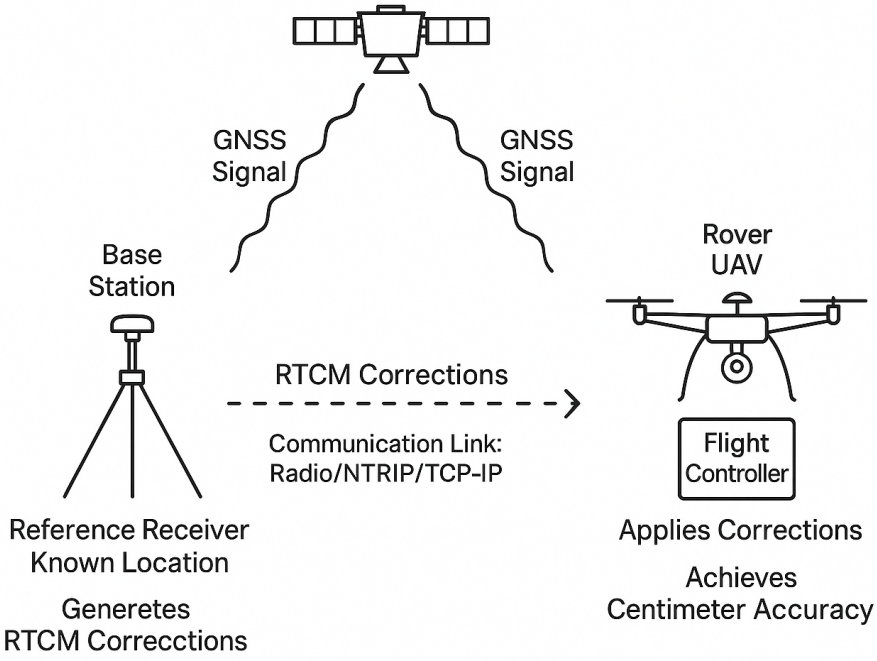

Figure 6: Overall RTK-enabled UAV positioning system architecture [48].

4.1.3 Rover Segment and UAV Integration

The rover portion contains a GNSS (Global Navigation Satellite System) receiver located at the UAV platform. This unit receives raw satellite data from the satellites overhead and then uses this received information to obtain an RTK (Real Time Kinematic)-fixed solution of its position in real time. In contrast to traditional single frequency GNSS receivers, modern multi-frequency GNSS receivers that support multi-constellation positioning provide improved robustness and reliability of resolving ambiguities in determining a fixed position relative to the rover [17].

The GNSS receiver communicates via serial communication protocol with the flight controller (i.e., UART or CAN). The high precision position estimates produced by the GNSS module are transmitted to the flight controller which then integrates these precise position estimates into its own navigation and control loop. Multi-GNSS receiver integration for UAV navigation and attitude estimation have demonstrated improvements in positioning robustness and navigation stability in experimental UAV systems [2].

4.1.4 Flight Control and Navigation Segment

The flight control component utilizes an ArduPilot firmware-based Pixhawk flight controller to implement the flight control component. The flight controller uses the GNSS position data, IMU data and other onboard sensor readings as inputs for state estimation and trajectory control. The ability to use RTK-corrected GNSS data will allow the controller to have high precision navigation capability during the landing phase, which can lead to less positional drift and greater consistency in landing accuracy.

Previous UAV navigation studies show tightly integrated navigation architectures combining GNSS based position information with the onboard flight control system provides enhanced navigation stability and operational dependability under a variety of flight conditions [10]. The system architecture utilized in this study includes a tightly integrated design to provide reliable communication between the GNSS position components and the flight control components.

4.1.5 Communication and Data Flow Architecture

For reliable correction data transmission that will support continued performance of RTK fix based positioning, the architecture utilizes a communications link dedicated to the transmission of RTCM correction message data from the base station or an external corrections network to the UAV rover receivers' correction data input. Data communications latency (i.e., delay) and data communications packet loss will impact the availability of the RTK solution; thus, reliability of data communications is a major design consideration [19].

There are three primary communication pathways in the entire data flow architecture: (1) receipt of GNSS signals by both the base and rover receivers from the GNSS constellation; (2) transmission of correction data from the base station or corrections network to the rover; and (3) transmission of navigation data from the rover to the flight controller. Each of these communication pathways is necessary to establish the operational foundation of the RTK-based positioning system.

4.1.6 Overview of GNSS Receiver Platforms

Beginning with a brief overview of the requirements of precision landing for Unmanned Aerial Vehicle (UAV), it has been noted that many of today's high-precision landing systems are based upon a multi-frequency Global Navigation Satellite System (GNSS) receiver with Real-Time Kinematic (RTK) capabilities. In recent years, advancements have allowed for multi-band GNSS chipsets which allow for precise positioning at the centimeter level and enable small, lightweight modules to be integrated into the payloads of UAVs. The ability of the GNSS receiver to support multi-frequencies (L1/L2/E5) as well as multi-constellations (e.g., GPS/BeiDou/Galileo etc.) improves the reliability of ambiguity resolution as well as the overall position availability compared to older single-frequency GNSS receivers [16, 17].

The objective of this thesis is to evaluate three RTK-capable GNSS receivers through experimentation: *simpleRTK2B ZED-F9P*, *simpleRTK2B ZED-F9R*, and *Here+ RTK M8P*.

All of these receivers utilize the u-blox F9-series multi-band GNSS chipset, providing carrier phase positioning capability, RTCM correction messaging, and flexibility in both the base and rover operational modes. Through comparative evaluations of multiple hardware platforms, an evaluation of positioning performance variability, correction messaging interoperability, and integration into UAV navigation architectures will be achieved.

Recent experimental studies on low-cost multi-frequency GNSS receivers indicate that current commercially available RTK modules can provide positioning performance comparable to traditional geodetic receivers when operating under favorable conditions, thus increasing the viability of utilizing high-precision UAV navigation systems. As such, evaluating these types of receivers in controlled experimental environments is critical to determine their usability in precision-landing applications.

4.1.7 simpleRTK2B ZED-F9P

The *simpleRTK2B ZED-F9P* receiver with Figure 7 used in this study is a well-established multi-band RTK GNSS development board intended for high-precision positioning applications, among others (i) UAV navigation, (ii) robotics, and (iii) surveying systems. The board contains the u-blox ZED-F9P GNSS module. The ZED-F9P module can receive multiple satellite signals from various satellite constellations (GPS, GLONASS, Galileo, and BeiDou) concurrently. Because the ZED-F9P module is capable of simultaneous multi-signal frequency reception, there are improvements in mitigating ionospheric error, improving the speed of resolving ambiguities, and enhancing the robustness of RTK positioning relative to traditional single-signal frequency GNSS receivers [28].

Figure 7: simpleRTK2B ZED-F9P receiver board (source: ArduSimple) [27].

Under conditions of reliable correction data and sufficient satellite visibility, the ZED-F9P board is capable of centimeter level positioning accuracy, especially when RTK-fix is achieved. The manufacturer's specifications show that the horizontal positioning accuracy of the ZED-F9P board will be less than one centimeter when using RTK corrections and

when the distance between the base station and rover is tens of km. However, without RTK corrections, the board's positioning accuracy will remain at a level of meters [27].

A primary benefit of the simpleRTK2B platform is its capability to switch between two modes of operation; as a base station, or as a rover receiver. When configured in base station mode, the receiver uses its known reference coordinates to calculate the RTCM correction messages necessary to correct for satellite clock errors, atmospheric delay, and orbital uncertainty. These correction messages are then sent to rover receivers through wireless telemetry, or network communication links. When configured in rover mode, the receiver utilizes these correction messages and the observed satellites to generate centimeter-level RTK fixed position solutions. The ability of the simpleRTK2B platform to operate as both a base station and a rover receiver provides the flexibility required by the researcher to evaluate multiple correction methodologies for UAV positioning architectures.

4.1.8 simpleRTK2B ZED-F9R

The simpleRTK2B ZED-F9R receiver with Figure 8 used in this study is a multi-band RTK GNSS module that has been designed to meet requirements that demand increased positioning robustness, specifically for applications that require the receiver to be able to function well while being dynamically moved. In contrast to the ZED-F9P module, the ZED-F9R utilizes an onboard IMU to provide a tightly-coupled GNSS–INS sensor fusion, thus improving the continuity of navigation and reducing the degradation in positioning caused by the temporary interruption of GNSS signals that typically occur in urban, semi-obstructed to open-sky transition, or partially obstructed flight environments [2].

Figure 8: simpleRTK2B ZED-F9R GNSS receiver board (source: ArduSimple) [29].

The receiver is capable of simultaneously tracking multiple GNSS constellations (i.e., GPS, GLONASS, Galileo, and BeiDou), and uses multi-frequency carrier-phase observations. Processing from multiple GNSS constellations will increase the number of available

satellites, and will also improve the reliability of ambiguity resolution, resulting in a more stable RTK positioning solution while in UAV flight operations [17]. Under favorable observation conditions, the ZED-F9R receiver will operate at centimeter-level positioning accuracy while in RTK mode, while also providing improved stability during dynamic maneuvers due to the onboard inertial navigation capability.

4.1.9 CubePilot Here+ RTK M8P

The CubePilot Here+ RTK GPS (Global Positioning System) is a UAV-specific RTK (Real-Time Kinematic) GNSS solution for UAVs (Unmanned Aerial Vehicles). It was developed for use as part of the autopilot systems and also for high-accuracy aerial navigation solutions. The Here+ RTK GPS is based on the u-blox NEO-M8P RTK-GNSS receiver and is presented as a typical base-rover positioning system as shown in Figure 9. It contains a GNSS receiver and antenna integrated with a magnetometer to make the integration with Pixhawk flight controller compatible. This combination of components makes installation and setup of the GNSS receiver much easier than the standalone development board version [30].

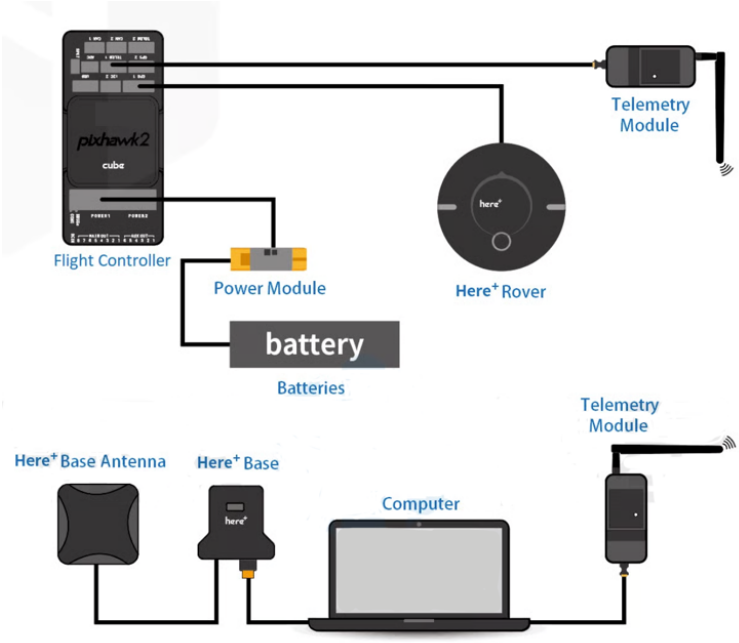

Figure 9: Hardware interconnectivity for the Here+ RTK M8P differential GNSS system. (source: CubePilot) [30].

Like all the other RTK-based receivers, the CubePilot Here+ RTK will support both multiple GNSS constellations and multi-frequency carrier phase positioning, which allows for centimeter level positioning when using the RTK fix. Multiple rovers receive correction from one single and enables them to receive centimeter-level positioning. It supports the tracking of signals from multiple satellite systems. These combinations are GPS, GPS & GLONASS, and GPS & BeiDou with a cold start of 26–29s and a hot start of 1s for each combination. We can use telemetry radio modules for the direct transmission of an RTCM (Real Time Correction Message) correction message from the base station to the rover

receiver. Therefore, the RTK positioning system can be rapidly deployed and does not require any additional communication hardware [18]. This type of integrated correction transmission system is especially beneficial for UAV field operations where both rapid system deployment and reliable communication are needed.

4.1.10 WiFi NTRIP-Based RTK Correction Transmission Using ESP32-XBee

Real-time transmission of RTK corrections to the UAV is required for providing accurate position information to a centimeter level of accuracy. The proposed system will employ a WiFi-based communication pipeline to deliver corrections to the GNSS receiver using the ArduSimple WiFi NTRIP Master module which is shown in Figure 10 as an embedded NTRIP client. The device connects to an NTRIP caster server through the available wireless network infrastructure and transmits the received RTCM correction stream to the GNSS rover receiver [31].

Figure 10: ArduSimple WiFi NTRIP Master used for RTK correction transmission [31].

The WiFi NTRIP Master utilizes an ESP32 microcontroller platform and implements IEEE 802.11 wireless communications to enable direct connections to the NTRIP caster server without intermediate computing systems. The module continuously receives RTCM correction streams from the correction service and transmits these streams through a serial communication interface or through telemetry radios such as XBee modules. This design will allow the UAV system to receive real-time correction data and maintain separate modular designs for the communication subsystems and onboard flight-control electronic systems.

4.2 Flight Controller Integration Using Pixhawk-4

The navigation and control functions of the UAV will be provided by an onboard flight controller called the Holybro Pixhawk-4 that utilizes either PX4 or ArduPilot firmware.

In our thesis, Holybro Pixhawk-4 flight controller is shown in Figure 11 which was running ArduPilot firmware. The Pixhawk-4 flight controller is built around a 32-bit ARM Cortex-M7 processor and therefore supports the real-time operation of flight-control algorithms, state estimation filter processes, and multi-sensor data fusion processes [32].

In addition to processing GNSS measurements, the Pixhawk-4 flight controller fuses data from multiple onboard sensors including inertial measurement units (IMU), magnetometer and barometer, which are used to determine the vehicle's state in real time while flying.

Figure 11: Pixhawk-4 flight controller used for UAV navigation and control [32].

Communication occurs between the Pixhawk-4 flight controller and the GNSS Rover Receiver via Serial UART interfaces using data formats compatible with NMEA, UBX, and MAVLink. The RTK corrected position information produced by the GNSS receiver is sent to the Pixhawk-4 flight controller and is then integrated into its onboard Extended Kalman Filter (EKF) to enable high accuracy navigation.

The availability of centimeter level accuracy RTK positioning allows for better tracking of a UAV's trajectory and increased repetition when attempting to land a UAV relative to stand-alone GNSS-based systems.

Multiple communication interfaces are available on the Pixhawk-4 flight controller (UART, CAN, SPI and Telemetry Ports) and can support the simultaneous connection of a GNSS receiver, correction telemetry radio and ground control communication module. These interfaces allow for the synchronization of communication between correction sub-systems, positioning sub-systems, and flight-control algorithms. Additionally, RTK status indicators (fix state, satellite visibility and positioning uncertainty) can be monitored in real time using ground control software interfaces; these status indicators can be useful for analyzing the performance of the positioning system.

As part of the proposed system architecture, the correction communication sub-system and flight-control sub-system will work together in a coordinated fashion. The WiFi NTRIP Master will retrieve correction data from the NTRIP Caster and send it to the GNSS Rover Receiver as RTCM messages. The GNSS Rover Receiver will compute RTK-corrected position estimates and transmit them to the Pixhawk-4 Flight Controller where they will be combined with the measurements taken by the Inertial Sensors to provide navigation and control of the UAV. The modular nature of the proposed system architecture ensures reliable correction transmission, stable positioning performance, and accurate trajectory control necessary for conducting UAV precision-landing experiments as described in this thesis.

5 Correction Sources and Configuration

5.1 Local RTK Base Station Setup

To allow for reliable high-accuracy positioning within the context of local Real-Time Kinematic (RTK) configurations, there needs to be an accurate determination of the position of a base station. This base station will provide the rover receiver(s) with correction data to facilitate precise positioning. The base station used in this research provided the rover receivers with precise positioning by utilizing a multi-frequency Global Navigation Satellite System (GNSS) receiver as the base station to generate RTCM messages for each of the satellites being tracked. The RTCM messages contained satellite clock error corrections, orbital corrections, and corrections for atmospheric delays caused by signal passage through the atmosphere.

Each rover receiver utilized in this research communicated with the base station via wireless communication to receive the necessary corrections to enable the rover receivers to achieve relative positioning accuracies in the range of centimeters [16, 17]. The local RTK base station was installed at a fixed site with no obstructions blocking the view to the sky to reduce multipath interference and to maintain a constant view of the satellites. Once initialized, the base receiver produced RTCM messages in real-time to be communicated to a local WiFi communication gateway utilizing an ArduSimple WiFi NTRIP Master module. The ESP32-based device functioned as a local NTRIP caster allowing rover receivers to obtain the correction data from the base station through a wireless communication link while eliminating the need for rover receivers to have internet access [31].

5.1.1 Local NTRIP Caster Configuration

Within the implemented architecture, the WiFi NTRIP Master created a local wireless hotspot to enable rover receivers to connect to the correction gateway directly over a wireless link. The Figure 12 is describing how the RTCM correction stream generated by the base station was then sent from the WiFi NTRIP Master to the ESP32-based NTRIP server. Upon arrival at the ESP32-based NTRIP server, the RTCM correction stream became accessible to rover receivers over a standard NTRIP connection. Rover receivers could then access the correction stream after authenticating with a set of predefined authentication parameters, which included the communication port number, mount point ID, user name, and password. After authenticating successfully with the defined parameters, each rover receiver continuously received correction data from the WiFi communication link and applied the RTCM corrections to the rover's position in real-time.

Local transmission of corrections offers several benefits to experimental positioning systems. First, the short distance between the base receiver and the rover receiver minimizes the difference in spatially-correlated atmospheric error; therefore, improving the rover's ability to resolve ambiguities and improve the positioning accuracy of the rover receiver. Second, the use of local NTRIP communication enables the rover receivers to operate independently of any other external networks; thus, providing the flexibility to perform experiments in both laboratory-controlled settings and field settings. Third, the system enables flexible configuration of correction update rates and communication parameters;

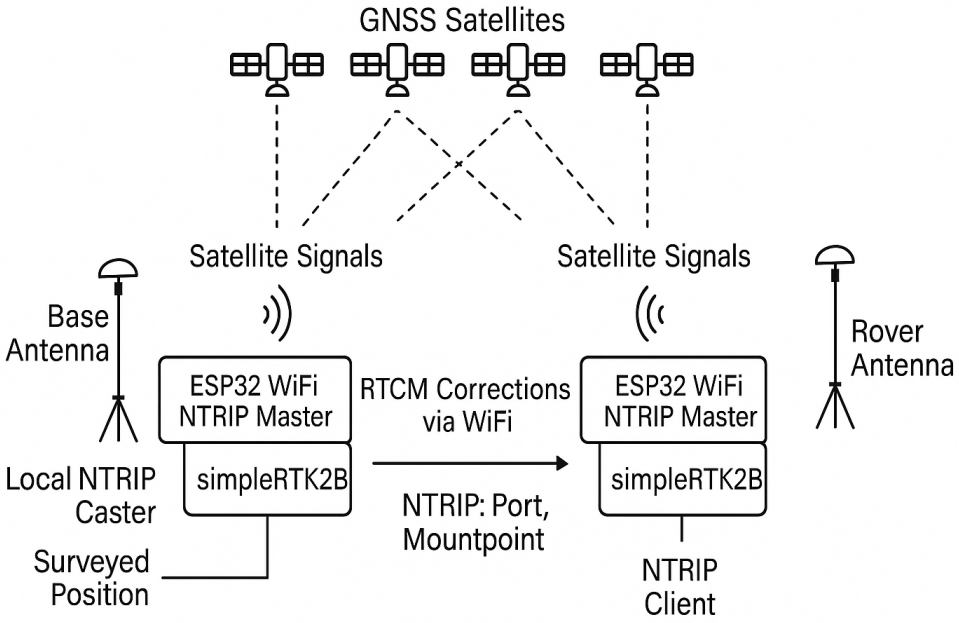

Figure 12: Local RTK base–rover communication architecture [48].

thereby, providing researchers with the capability to systematically evaluate how communication affects positioning performance.

Consistent delivery of corrections is crucial to the maintenance of RTK fix solutions during UAV operations. Interruptions to communication, losses of packets, or variations in latencies can result in temporary degradations of positioning performance; therefore, resulting in float or standalone solutions. Literature reviews related to communication systems for RTK indicate that reliability in correction dissemination plays a key role in maintaining consistent positioning performance at the centimeter level; especially when considering mobile navigation environments [19]. As such, the local RTK base-station configuration developed in this research served as a controlled baseline correction infrastructure against which network-based correction services can be compared.

5.2 SAPOS Correction Service

In addition to correction data created in the field, the experimental setup was designed to obtain network-based RTK corrections from the German Satellite Positioning Service (SAPOS) (AdV), which is a service provided by the surveying authorities of the German federal states. SAPOS delivers nationwide high-precision positioning services through a network of continuously operating GNSS reference stations that collect satellite signal information and produce space-modelled correction data [34].

These correction streams are distributed via the NTRIP communication infrastructure as part of the SAPOS High-Precision Real-Time Positioning Service (HEPS), allowing users of registered RTK-capable GNSS receivers to access real-time RTCM correction data. In order to access the service, a unique set of login credentials assigned during the SAPOS registration process needs to be used for authentication. The Figure 13 is showing how a rover GNSS receiver uses the ESP32-based WiFi communication module, which has been

configured as an NTRIP client, to connect to the SAPOS NTRIP caster. After successful authentication using the provided username and password, the rover continues to receive correction data from the selected mountpoint, and then applies the corrections to generate high-precision position estimates.

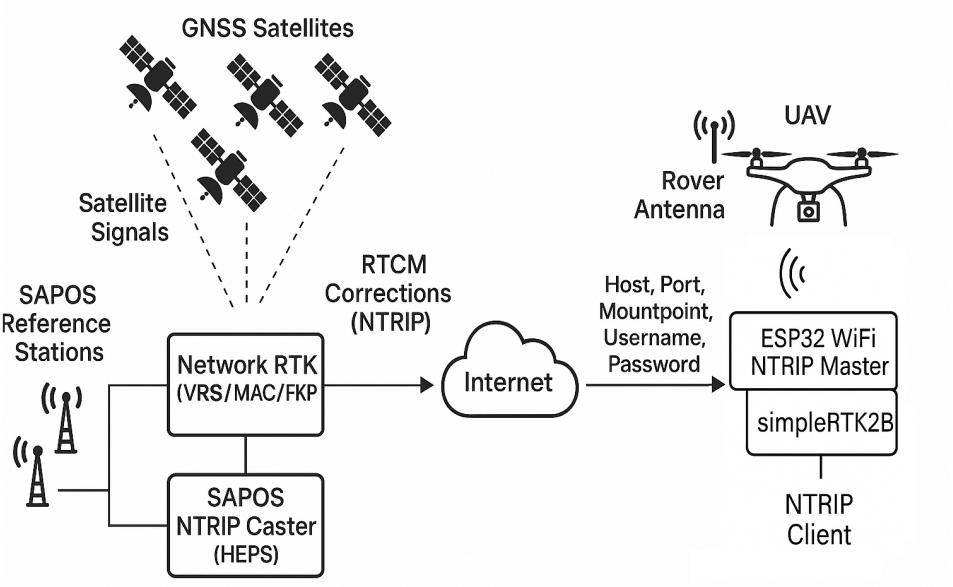

Figure 13: Network RTK of SAPOS reference-station networks [48].

Advanced processing techniques, including Virtual Reference Station (VRS), Master–Auxiliary Concept (MAC) and area correction parameter (FKP), have been employed in network RTK services like SAPOS to model spatially correlated positioning errors across vast geographic areas. These techniques create localized correction streams that are tailored to the rover's location and therefore improve the positioning performance relative to long-baseline single-base RTK solutions [14, 25]. According to the SAPOS service specifications, the HEPS correction service should provide horizontal positioning accuracies ranging from 1 to 2 cm when optimal observation and communication conditions exist [34].

Using SAPOS network-based correction services also provides several operational advantages compared to local base station installations. Network RTK removes the necessity for installing and maintaining local reference stations and provides wide-area coverage, thereby enabling UAV positioning operations across large geographic areas. However, there is a dependency on the availability and reliability of the internet connection and communication infrastructure when delivering corrections via the network. This could lead to temporary connectivity loss or changes in network latency, which in turn could affect the availability of corrections and hence the continuity of RTK fix solutions during UAV operation.

5.3 Base–Rover Interchangeability Analysis

The conventional operational setup for RTK GNSS positioning systems assigns one receiver as a stationary reference base station (the "base") and a second receiver as the rover

platform which generates real-time position estimates. Many commercial RTK capable modules currently have the capability to function in various operational modes allowing them to be used interchangeably as either a base receiver or a rover receiver. Assessing the interchangeability of base and rover receivers will help identify the degree of flexibility and compatibility of hardware in RTK positioning systems as well as the level of consistency in positioning performance when different receiver platforms are used to obtain corrections from the same correction infrastructure.

Within the experimental design of this research, several multi-frequency GNSS receiver platforms were assessed in interchangeable base-rover configurations. Each receiver was set up to operate as a base receiver while the other receivers were operating as rovers and receiving RTCM correction streams from either a local NTRIP server or through network RTK services. This type of experimental design allowed for a systematic assessment of how positioning performance varies based upon the type of receiver hardware being used as the base receiver and if the use of a combination of receiver hardware (heterogeneous) would result in reliable RTK-fix solutions.

5.3.1 Experimental Setup

The interchangeability of receivers was examined using several types of RTK capable GNSS receiver platforms; specifically, ZED-F9P-based and ZED-F9R-based receivers as well as Here+ RTK M8P kits. For each experimental configuration, one receiver was positioned at a fixed reference point to produce RTCM correction messages while the rover receiver was mounted on the UAV or a moving test stand to assess positioning performance. Once the measurement sequence was complete, the base and rover functions were switched and the experiment was repeated under identical environmental and communication conditions.

All receiver configurations were run under identical environmental conditions (i.e., antenna installation, correction communication interface, and satellite visibility); the rover receivers were also configured to receive correction streams from both the base receiver(s) and network RTK correction services to examine the impact of correction infrastructure on interchangeability performance. The metrics used to assess performance included RTK-fix availability, horizontal positioning accuracy, positioning stability during movement, and correction initialization convergence time.

5.3.2 Effect of Hardware Characteristics on Interchangeability

While RTK positioning theoretically relies solely upon the quality of the correction data and the geometric relationship between the receiver and satellites, the performance of a given RTK positioning system may also be influenced by the receiver hardware characteristics (e.g., signal tracking sensitivity, observation noise levels, antenna interface quality). Some studies regarding low-cost multi-frequency GNSS receivers suggest that differences in receiver hardware performance may adversely affect the quality of observations obtained and/or the reliability of resolving ambiguities [9], especially in difficult signal environments. Thus, assessing the interchangeability of receiver hardware under real world conditions is an effective way to determine the compatibility of hardware among various RTK positioning architectures.

Experimental results indicated that modern multi-frequency GNSS receivers exhibit similar positioning accuracy when operated in interchangeable base-rover configurations, as long as the quality of correction data and reliability of communications remain constant. Multi-GNSS carrier phase positioning methods can resolve integer ambiguities reliably across heterogeneous receiver pairs and thus enable stable centimeter-level positioning solutions under optimal observation conditions [17] . However, the potential exists for slight differences in RTK initialization times and availability due to variations in antenna configurations, receiver firmware processing approaches, and correction message processing techniques.

6 Software Configuration and Data Handling

6.1 GNSS Configuration Using u-center

This study utilizes receivers from the simpleRTK2B product family that utilize the u-blox ZED-F9P chipset and configured these receivers using the u-blox *u-center* software environment for GNSS receiver configuration and performance evaluation. As stated above, the u-center software provides a number of features including a graphical interface for receiver configuration, firmware management, performance monitoring, and real-time navigation analysis [35].

6.1.1 u-center Installation and Initial Setup

As previously mentioned, the receiver configuration process starts with the installation of the correct version of the u-center software for the u-blox F9-series receivers [35]. After installing the software, the receiver is physically connected to the host computer via the USB interface labeled POWER+GPS and the correct COM port is can be chosen as shown in fig 14. With a valid connection, the u-center software will present real-time satellite observations, navigation status indicators and signal strength information. It is important that the antenna has been placed properly with clear sky visibility to maintain a stable track on satellites and to enable accurate positioning initialization.

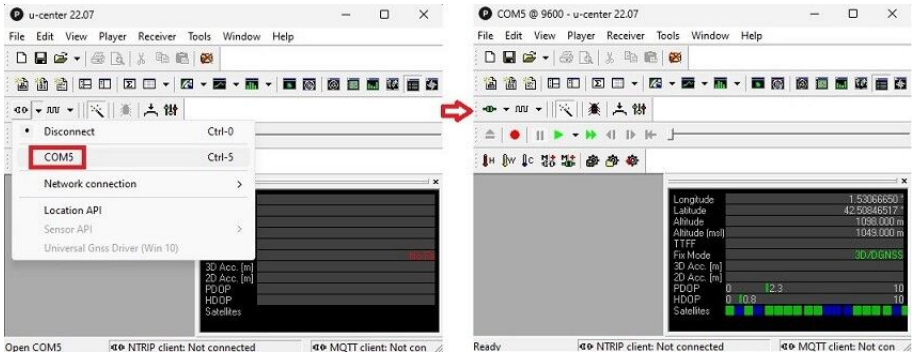

Figure 14: Set-up of receiver connection in u-center [35].

The graphical interface provided by u-center allows for the activation of several different types of visualization panels such as a view of the satellite signal strengths, a geographic positioning display and a window for viewing navigation data. These visualization tools provide immediate feedback about whether the receiver is properly connected to the network, how many satellites are visible and what type of positioning status the receiver is currently in, thereby allowing the experimenter to verify the proper functioning of the receiver hardware prior to configuring the receiver.

6.1.2 Firmware Verification and Update

In addition to verifying that the receiver is properly connected and providing the expected level of positioning performance, it is necessary to verify the firmware version installed in

the receiver to ensure that it is compatible with the intended operational requirements [9]. The version of the firmware currently installed in the receiver can be determined using the *UBX-MON-VER* message interface in the u-center Message View panel.In fig 15, we can see that firmware installed is 1.32 and in our device we have used firmware version 1.13. The different versions of the firmware provide different update-rate capabilities and levels of correction-service compatibility; for example, firmware version 1.13 provides an update rate of up to 10 Hz, which would be sufficient for the high-frequency update requirements of a UAV navigation system.

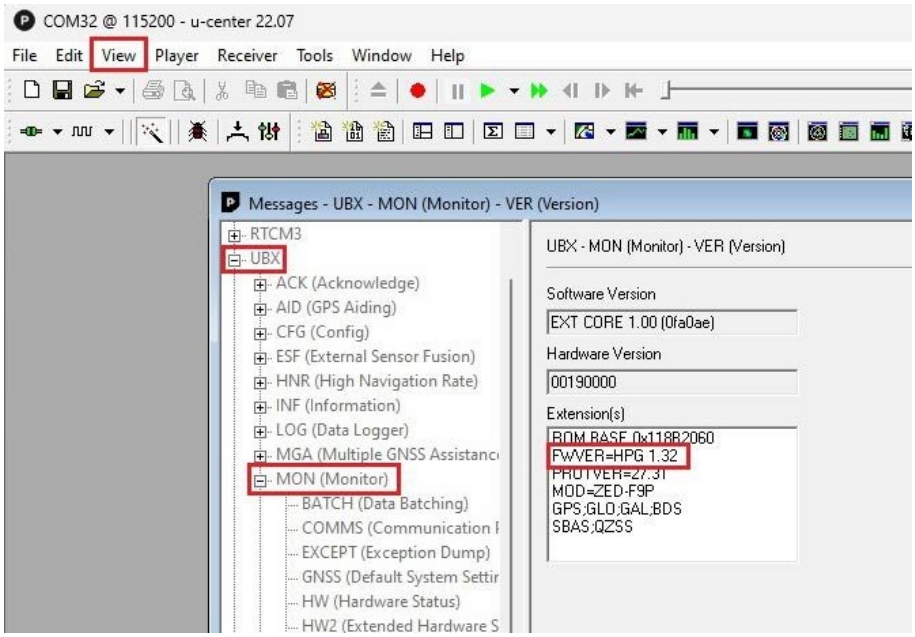

Figure 15: Firmware verification in u-center [35].

If necessary, firmware updates can be performed through the *Tools → Firmware Update* menu item. This menu item enables uploading the new firmware file to the receiver using the previously defined communication interface. Following a successful update, the receiver is restarted and the firmware version is again checked to confirm that the firmware was successfully updated.

6.1.3 Base Station Configuration

The next step in the configuration process is to configure the receiver as a base station. To accomplish this task, the receiver must first be configured to generate RTCM correction messages using one of two methods: the automatic survey-in method or the fixed-position method [17]. The automatic survey-in method allows the receiver to estimate its approximate coordinates by taking an average of the satellite observations taken during a predetermined observation period. This method is most suited to experimental situations where precise reference coordinates are not available. During survey-in initialization, the user defines the minimum observation time and required position accuracy criteria through the *UBX-CFG-TMODE3* configuration interface. When the specified accuracy and time criteria have been met, the receiver automatically switches to time-mode operation and generates RTCM correction messages. In fig 16, we can see that our base station will be

automatically surveyed for minimum of 180s and required positional accuracy is consider as 2 m.

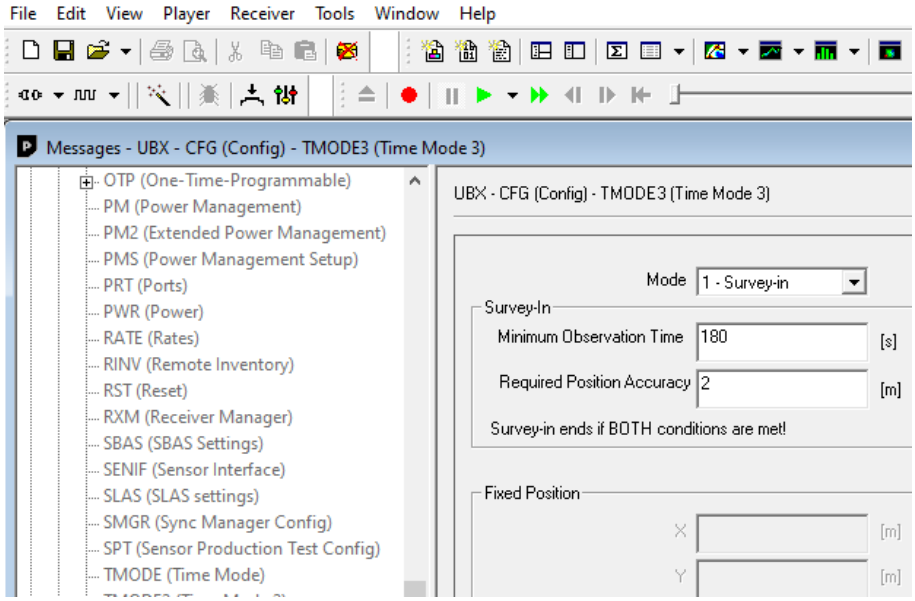

Figure 16: Survey-in for base station in u-center.

For applications requiring consistent absolute positioning accuracy across multiple sessions, the fixed-position method is generally preferable. In this configuration, the known coordinates of the antenna are manually entered into the receiver's configuration interface. This enables the base station to generate corrections relative to a stable geodetic position. Fixed-position configuration eliminates coordinate drift between power cycles and enables consistent centimeter-level absolute positioning accuracy. The fixed-position parameters are configured using the same *UBX-CFG-TMODE3* interface. However, instead of selecting time-mode operation, the user selects fixed-mode operation and enters the antenna coordinates in terms of latitude, longitude, and altitude in the corresponding fields.

Following selection of the base-station operating mode, RTCM correction messages must be enabled for transmission. This is accomplished through the *UBX-CFG-MSG* configuration interface, where the user activates the required RTCM message types for the desired communication interface (typically UART2 or USB). The commonly recommended RTCM messages include message types 1005, 1074, 1084, 1094, and 1230, which contain reference-station information and multi-constellation carrier-phase observation data. Additionally, communication parameters such as baud rate and output protocol must be configured using the *UBX-CFG-PRT* interface to ensure that the correction messages are transmitted correctly.

Finally, the configuration is written to receiver memory using the *UBX-CFG-CFG* command, so that the receiver maintains the base-station configuration settings upon subsequent power cycling. Ongoing monitoring of the survey-in status and correction-generation process can be performed through the *UBX-NAV-SVIN* status interface, which indicates the current survey duration, position uncertainty, and survey-completion status.

6.1.4 Rover Receiver Configuration

When configuring the receiver as a rover, the receiver must be configured to receive RTCM correction messages and perform RTK positioning calculations. The configuration process begins by either loading a predefined rover configuration profile or manually defining the receiver parameters using the receiver's configuration message interface. The communication parameters, such as the UART baud rate, must be defined to ensure compatibility with the telemetry radios or communication modules that transmit correction data. Typically, a rover configuration includes defining UART2 to operate at 115200 bps, and activating the support for the RTCM3 input protocol.

Additionally, certain constellation and augmentation system parameters may be set to optimize the navigation performance of the receiver. For example, deactivating the SBAS augmentation system can eliminate position jumps during short correction interruptions, and deactivating unused constellations can increase the navigation update rate without causing communication buffer overflow. The navigation rate parameters are configured using the receiver configuration interface to achieve the desired update frequency, which can vary from 1 Hz to 10 Hz depending on the specific application requirements.

Following the definition of the configuration parameters, they are written to receiver flash memory using the Save Config function to ensure that the configuration remains active following a power cycle. At this point, the receiver begins to operate in rover mode, continuously monitoring the incoming correction streams and attempting to resolve the integer ambiguity to achieve RTK-fixed positioning status.

6.1.5 NTRIP Correction Reception

The u-center software provides an integrated NTRIP client interface for receiving RTCM correction data from either a local base station or an internet-based NTRIP correction service. We have used SAPOS for NTRIP correction which can be seen in fig 17 by providing already known connection parameters such as the server address, communication port, username, password, and mountpoint were configured using the u-center NTRIP client interface. Upon establishing a valid connection to the server, the rover receiver begins to receive RTCM correction messages through the communication interface and attempt to calculate RTK-fixed position solutions. The success of receiving correction data is indicated by a transition from standalone or float mode to RTK-fix mode, along with the indicators of centimeter-level positioning accuracy.

Ongoing monitoring of the RTK status, satellite tracking conditions, and positioning accuracy is performed using the navigation status panels that are accessible through the u-center interface. By performing ongoing monitoring, the experimenter can identify rapidly any communication or configuration issues that may impact the positioning performance of the system.

6.2 Pixhawk and ArduPilot Configuration

The process of integrating the GNSS receiver with the flight control system is an important part of achieving accurate positioning at the centimeter level for UAVs. For this research,

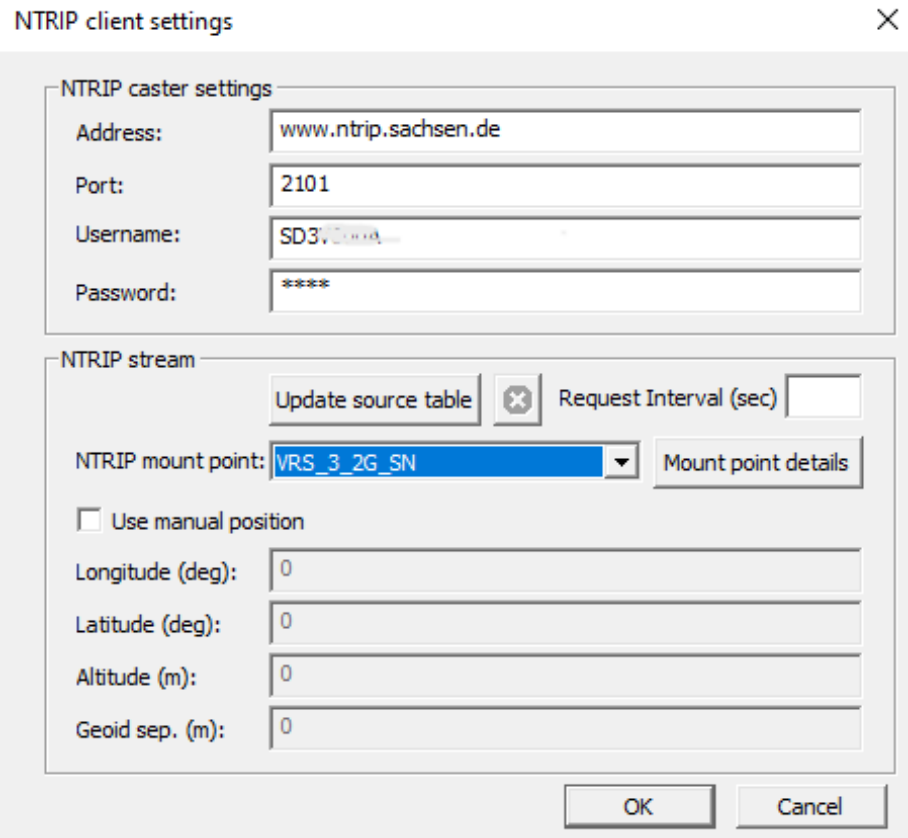

Figure 17: NTRIP client configuration in u-center.

the Pixhawk 4 flight controller that runs ArduPilot was used as the primary autopilot platform. The simpleRTK2B receiver powered by the u-blox ZED-F9P GNSS module was configured to provide high-frequency positioning updates and to accept RTK corrections; it was then connected to the autopilot system [37].

6.2.1 Preparing the GNSS Receiver for Autopilot System Integration

Before integrating the GNSS receiver with the autopilot system, the GNSS receiver was first configured using the u-center software to verify that it meets the requirements of ArduPilot's communications protocols. Next, the receiver's firmware was checked to verify its functionality using firmware version 1.13, which enables positioning update rates of up to 10 Hz, providing sufficient data for dynamic UAV operations. A pre-configured configuration profile was next downloaded into the receiver to enable the generation of high-frequency navigation updates and proper message transfer to the autopilot system. This configuration profile specified a positioning update rate of 10 Hz, and activated the UBX-PVT (position, velocity, time) navigation message output, which provided the autopilot with real-time position (latitude, longitude), elevation (altitude), velocity and fix-status information. Following the downloading of the configuration file, the receiver's settings were stored in non-volatile flash memory to ensure they would remain intact even after power cycling. The above described steps ensured that there would be a stable exchange of data between the GNSS receiver and the flight controller during UAV operation.

6.2.2 Configuration of Autopilot Parameters

Once the GNSS receiver had been prepared, the Pixhawk flight controller was configured using the Mission Planner ground control system. The flight controller was connected to the host computer via USB communication, and the autopilot firmware version was compatible with ArduPilot version 4.1 or greater to ensure parameter compatibility and reliable multi-GNSS support.

Using the Mission Planner's parameter configuration interface, several system parameters were modified to enable the use of an external GNSS receiver and RTK-based navigation. Use of the internal compass was disabled when either external heading or multiple receiver configurations were being used to prevent conflict between sensors. Additionally, GPS automatic configuration features were disabled to permit manual configuration of the communication parameters and receiver settings. The external GNSS receiver was designated as the primary source of navigation data, and the GPS update rate was adjusted to match the receiver's output frequency.

Parameters for serial communication were configured to ensure reliable communication between the GNSS receiver and the autopilot's telemetry interface. The communication baud rate was established to correspond to the receiver's output configuration, commonly 460800 bps or 115200 bps based upon the selected interface. The serial protocol was configured to enable receipt of GNSS message inputs, permitting the autopilot to continuously receive navigation solutions generated by the receiver. Upon completion of parameter modifications, the updated configuration was stored in the autopilot's memory, and the system was rebooted to apply the new configuration.

6.2.3 Hardware Integration of the GNSS Receiver and Autopilot System

The GNSS receiver that had been previously configured was then physically connected to the Pixhawk flight controller using the dedicated telemetry interface cable. The JST-GH telemetry cable connected the receiver's UART interface to the TELEM1 port of the Pixhawk, enabling two-way communication between the two devices can be seen in fig 18. for our research,TELEM1 port was kept free, instead we used UART & I2C B port for connecting our RTK device to the Pixhawk and indoor(semi-obstructed) gps was plugged in GPS MODULE slot. we have used Properly installed antennas and unobstructed access to the sky were necessary to ensure reliable satellite signal reception during operation. Upon energizing the autopilot system, the ground control system automatically detected the presence of the external GNSS receiver and displayed navigation data through the MAVLink telemetry interface.

Correct connectivity of the GNSS receiver and correctness of the navigation data received by the autopilot system were verified using the Mission Planner MAVLink Inspector interface, where the real-time GPS message stream could be viewed. Positioning data displayed in Mission Planner was cross-checked with positioning data observed in the u-center software to confirm proper integration of the GNSS receiver and data integrity of the data transmitted to the autopilot system.

Figure 18: simpleRTK2B and Pixhawk configuration [37].

6.2.4 Integration of RTK Corrections

To achieve centimeter-level positioning accuracy, the GNSS receiver must be able to receive RTK correction messages, which may originate from either a local base station or an internet-based NTRIP correction service. Once correction messaging has been enabled, the receiver will process the incoming RTCM correction stream and attempt to resolve the integer ambiguity. Receipt of valid corrections is confirmed by the change of the GNSS positioning status from standalone mode to RTK-float and ultimately to RTK-fixed status as viewed in the fig 19. Here GPS 1 is our indoor(semi-obstructed) simulated lab GPS which shows correction status as 3D Fix.

Upon transitioning to RTK-fixed mode, significant improvement in positioning accuracy occurs, with positioning errors in the horizontal plane reduced from meter-level to centimeter-level precision. During UAV flight experiments, continuous monitoring of the fix status, satellite geometry, and correction reception stability are performed through both Mission Planner and u-center monitoring interfaces to ensure reliable operation of the RTK-enabled UAV system [37]. Therefore, proper configuration of the GNSS receiver, autopilot parameters, and correction communication paths is a prerequisite for consistently achieving high-precision navigation performance in RTK-enabled UAV systems.

6.3 Data Logging and Processing

Investigating and correctly-reporting RTK performance relative to operational UAV characteristics hinges upon the persistent recording, clever archiving, and repeatable processing of GNSS observations. Modern UAV navigation research argues that all validation experimentation should be performed upon traceable pipelines of information, not snapshots of measurement [6]. We plugged in a modular real-time logging subsystem into

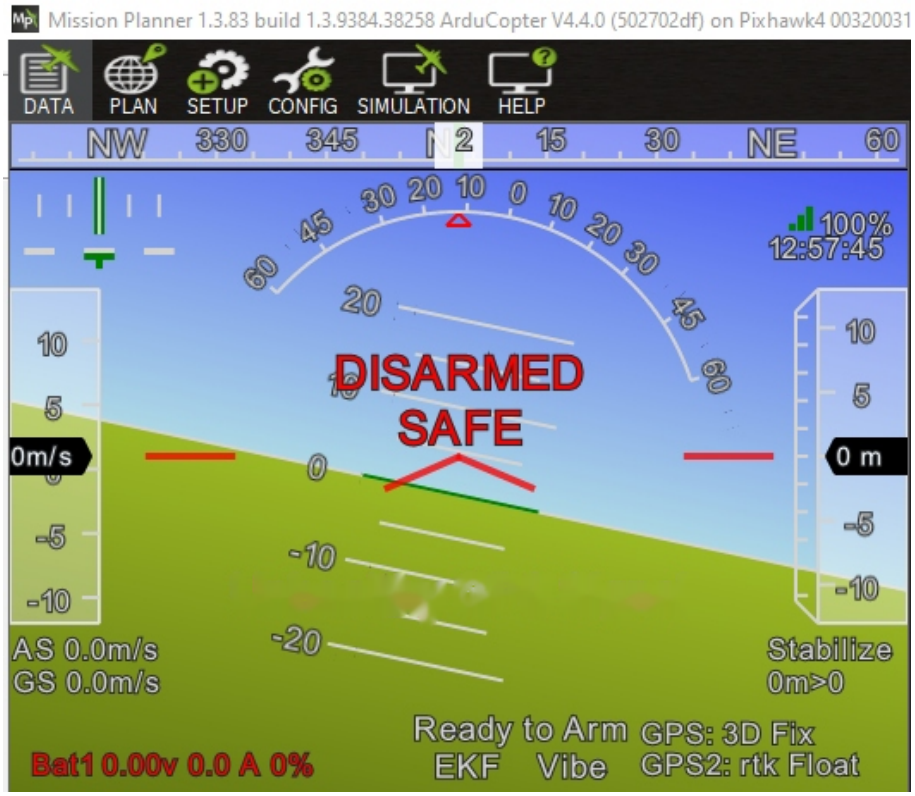

Figure 19: GPS and GPS2 correction status in mission planner.

the TUC Hangar Cloud in order to begin to respond to these ideals of reproducibility, synchronization, and statistical validity of all positioning experiments.

The architecture is of a layered system. In fact:

1. GNSS Data Acquisition Layer - Base and Rover Receivers
2. Data Ingestion and Preprocessing Layer
3. Relational Database Persistence Layer
4. Server API Layer
5. Frontend Layer

Layered structures have been extensively used in testbeds of UAV navigation to improve modularity and maintainability. A layered structure has the advantages of ensuring separate responsibility and fault isolation, and the scalable design of the acquisition, storage, and visualization component of each layer.

The base station provides continuous updating about status regarding corrections that will be applied such as survey-in convergence and fixed-mode coordinates of geodetic reference fix. The rover receiver likewise provides navigation data and metadata that includes base geodetic position, altitude and fix-quality indicator. These observations are made into structured descrete units of full geodetic coordinates as itemised in WGS84, in the format used in the GNSS positioning community [17]. Each observation is timestamped in UTC and made into decoupled instances conformant with existing ontologies; this allows temporal traceability as every observation comes from a particular point in time.

Such tracing is crucial where the appraisal of RTK as a part of the positional hierarchy in a larger overall framework relies on quality and bona fides of the piece of information in static conditions, and in rapidly changing UAV conditions and dynamics [6, 7].

6.3.1 Real-Time Data Acquisition

GNSS data acquisition in real-time is carried out through continued serial communication between the receivers and the processing workstation. As stated in the GNSS receiver architecture principles, real-time carrier-phase processing requires continued data streaming to prevent ambiguity re-initialization.

Survey-in or fixed-position status is monitored for the base station to determine when reference coordinates are stable enough to define. Survey-in convergence behavior is directly related to the consistency of absolute positioning of the rover [6]. Manually defined reference coordinates in fixed mode provide centimeter level repeatability of reference coordinates over multiple power cycles [17].

For rover operation, the navigation message provides:

- geodetic location (latitude and longitude),
- ellipsoidal elevation (altitude),
- fix quality indicator,
- satellite tracking status.

The fix-quality indicator is mapped to positioning states such as standalone GNSS, DGPS, RTK Float, and RTK Fixed. Only measurements with valid fix states are persisted to ensure the integrity of the data set. Studies on RTK reliability emphasize that float solutions can cause significant deviations from the true position and should be differentiated from fixed solutions during performance analysis [6].

The continuous data acquisition pipeline minimizes buffering latency and enables the positioning information to be available immediately for monitoring and statistical analysis.

6.3.2 Data Storage and Management

All GNSS observations are saved in a PostgreSQL relational database for providing structured persistence and reliable transactions. Separate tables are maintained for base station reference coordinates and rover trajectory data. Each table entry contains:

- Universally Unique Identifier (UUID),
- Timestamp (UTC),
- Latitude and longitude,
- Altitude,
- Fix Status,

- Device Identifier.

On this UUID being a simple remote identification in UAV instances of distributed locations.

Triggers built into the database can emit notification events that have been inserted into the database. For real-time positioning systems, event-driven architectures are preferable to reduce polling overhead and enhance scalability. The notification mechanism ensures that backend services can react to new GNSS observations without incurring significant processing latency.

The storage design serves for:

- Retrieve the most recent positioning state of the rover,
- Filter data by time range,
- Reconstruct historical trajectories of the rover,
- Export the dataset for off-line analysis.

Such information persistence structure facilitates synchronized comparison of GNSS measurements and flight controller telemetry logs during experimental evaluation [4].

6.3.3 Real-Time Visualization and Monitoring

A web-based monitoring interface was incorporated into the Hangar Cloud environment wherein live supervision of GNSS system status can be performed. Authentication is employed whereby backend services expose authorized API endpoints to allow retrieval of latest and historical positioning records.

The system visualizes:

- Current location of the rover,
- Records of the rovers historical trajectory,
- Reference coordinates of base stations,
- Classification of RTK fix status.

Differentiating between RTK Float and RTK Fixed states is essential for operational UAV safety and faithfulness for landing procedures [6]. Immediate monitoring hence enables immediate verification of centimeter-level positioning before commencing precision landing procedures [4].

Separating acquisition processes from visualization confers more log continuity when faced with frontend glitches, thus making longer in-field experiments more robust.

6.3.4 Relation to Accuracy Evaluation

The logging framework we implemented bears direct relevance to quantitative accuracy assessment of RTK positioning performance. High-precision UAV application necessitates statistical determination as opposed to merely visual inspection of instantaneous coordinates [3, 6].

The structured dataset permits computation of:

- Mean Positioning Error,
- Standard Deviation of horizontal and vertical positioning errors,
- Ratio of RTK Fix Availability,
- Time to achieve convergence from a float to a fixed solution ,
- Static Repeatability Metrics ,
- Dynamic Trajectory Stability.

Time-range filtering allows subclassing of segments of the flight e.g., survey-in initialization, static validation, dynamic flight, landing etc. Multi-GNSS RTK performance studies emphasise ambiguity resolution success rate and environment on positioning reliability [17].

Storage of the basestation reference coordinates independently can be used to corroborate how stable the reference is, which is how we can interpret shift in the rover position [6].

In conclusion, the developed data logging and processing architecture forms the methodological basis for reproducible, statistically valid assessments of RTK accuracy in UAV precision landing experiments.

7 Experimental Methodology

7.1 Test Environment and Setup

To evaluate the performance of RTK-enabled UAVs for precise positioning, it is crucial to have a methodical and replicable experimental approach. For high-accuracy GNSS experiments, accurate reporting of the test environment, equipment configuration and the correction infrastructure is needed to ensure scientific replication and statistically valid conclusions [38, 39]. In this section we describe the physical environment in which the experiments were carried out, the hardware configuration, and the correction transmission architecture.

7.1.1 Physical Experimental Environment

To evaluate RTK position estimation under varied signal conditions we evaluated RTK performance in 2 distinct physical test environments; semi-obstructed laboratory and open-sky outdoor.

The first test environment was the TUC indoor(semi-obstructed) drone laboratory and had the GNSS antenna placed outside the laboratory building, near a window opening. the remaining equipment (receiver) was housed indoors. The surrounding laboratory building structure and adjacent structures resulted in partial blocking of the satellite signal and multi path reflections. Semi-obstructed environments such as those tested here are well-known to adversely affect carrier phase measurements, and reduce the quality of ambiguity resolution due to signal diffraction and reflection effects. We intentionally selected this semi-obstructed configuration to assess the RTK system's ability to operate under sub-optimal signal conditions typical of urban or partially obstructed environments.

Due to the close proximity of nearby structures, the satellite signals experienced temporary blockages during low elevation angles and exhibited higher levels of multi-path susceptibility than open-sky conditions. Consequently, variability in fix availability and convergence times were noted relative to open-sky testing conditions. By testing in this semi-obstructed configuration, we were able to determine how sensitive the RTK system is to shading from structural elements and environmental interference.

The second test environment consisted of an open-sky area located on the university campus. The base station and rover antennas were deployed in a manner that provided unobstructed sky views and minimal surrounding vertical structures. Open-sky conditions provide optimal satellite geometry and lower levels of multi path interference, which allow for determination of the RTK system's best case performance. multi-constellation tracking was utilized, and a stable satellite count greater than 18 satellites was normally achieved during testing.

Comparing the two test environments will enable a quantitative analysis of the RTK system's reliability, fix availability ratio, and positional stability under both extreme (constrained) and ideal (open-sky) signal environments. Utilizing both test environments ensures that performance analysis is not limited to ideal conditions, but rather includes practical operating conditions for UAV precision landing systems.

7.1.2 Hardware Configuration

A base-rover architecture using two multi-frequency GNSS receiver modules was implemented. The base receiver module was designed to generate RTCM (Real Time Correction Message) correction data for real-time kinematic positioning. The advantages of using a dual-frequency RTK receiver include quick determination of carrier phase ambiguity, which enables highly accurate positioning [39, 40].

Depending upon the requirements of each experiment, the base receiver was configured to operate in either "survey-in" mode or "fixed-position" mode. When the receiver was configured to operate in "survey-in" mode, the receiver's reference coordinates were determined by calculating the average of carrier phase measurements over a pre-determined "convergence time". Conversely, when the receiver is in "fixed-position" mode, the receiver's reference coordinates are known in advance to allow for consistent coordinate determination across multiple iterations of the same experiment [38].

The rover receiver module was mounted on the UAV and had a navigation update rate of 10Hz to satisfy the need for sufficient temporal resolution during all phases of UAV motion including during landing [42]. The GNSS antenna was permanently mounted on the UAV structure so that the geometric relationship between the antenna and the aircraft remained constant from flight to flight.

Two different architectures for transmitting corrections to the rover were evaluated:

1. A local, WiFi-based NTRIP (Networked Transport of RTCM via Internet Protocol) server.

2. Network-based RTK correction services. For example: SAPOS.

RTK correction services based on a network utilize VRS (Virtual Reference Station) principles to correct GNSS receiver errors over vast areas [41] . By evaluating both local and network-based RTK correction services, the potential delays associated with receiving corrections, the likelihood of achieving a fix and the reliability of the solution under varying infrastructure conditions can be determined. Based on the experimental observations,set up of local base always better, as it gives better positional accuracy compared to network based corrections, although we need to consider the location of base station. For less complexity and easy to use, Network based RTK correction is more suitable.

7.2 Test Scenarios

To test the RTK-enabled UAV position estimation framework thoroughly, a number of experimental scenarios have been developed and will be tested for their ability to accurately estimate the UAV's position. Each scenario has been developed to test different aspects of the system; specifically, to test the performance of various correction infrastructures, to determine how well the system performs under different types of hardware configurations, and to test the system's robustness under different types of environmental conditions.

In addition, each experimental configuration will be performed at least once under semi-obstructed laboratory-adjacent conditions and at least once under fully-open sky campus

conditions. During all experiments, the UAV's position will be logged continuously during the experiment and then post-processing will be performed to generate error statistics for horizontal (H) and vertical (V) positioning errors as well as for three-dimensional (3D) positioning errors.

7.2.1 Scenario Group 1: Network RTK Using SAPOS Corrections

The first group of experimental scenarios will investigate the performance of RTK-positioning using SAPOS corrections over the internet. In this case, the SAPOS corrections are transmitted over the internet to the UAV's rover module where they are received using NTRIP authentication credentials.

The primary goal of this group of experimental scenarios is to examine how different rover modules affect positioning performance when the quality of the corrections remains constant. To accomplish this goal, four different rover modules will be evaluated. These rover modules include:

- Unit 1: ZED-F9P
- Unit 2: ZED-F9P
- ZED-F9R
- Here+ RTK M8P

All of these rover modules will be connected to a Pixhawk flight controller so that the results can be compared to those obtained using a typical UAV system.

In the semi-obstructed laboratory-adjacent environment, the GNSS antenna will be located outside but adjacent to the laboratory window with the remainder of the receiver hardware located inside. This location introduces some satellite shading and increases the likelihood of multipath errors.

Conversely, in the open-sky campus environment, there should be no obstacles blocking the direct line-of-sight to the satellites and thus, no multipath errors. Thus, it will be possible to evaluate the following factors using these two locations:

- The sensitivity of each of the different rover modules to satellite shading,
- The continuous nature of the RTK fixes,
- How rapidly the accuracy degrades under the influence of multipath errors,
- How stable the positioning performance is between two identical ZED-F9P units.

Thus, the results of this group of experimental scenarios will help to determine if the differences in positioning performance are caused by the differences in the hardware used or by the differences in the environmental conditions. Although we have tested the Here+ RTK M8P Rover and have found fix status, accuracy are not measured in this thesis.

7.2.2 Scenario Group 2: Here+ M8P as Reference Base Station

In the second group of experimental scenarios, the effect of the quality of the base station on the rover's positioning accuracy will be investigated. For this group of experimental scenarios, one CubePilot Here+ RTK GPS receiver, which operates in survey mode, will be used as the reference base station. The rover modules that will be tested include the ZED-F9P and the ZED-F9R. The rover modules(u-block NEO-M8P) was also being tested for RTK fix status although no accuracy was not tested in this scope of study.

When we use the CubePilot Here+ as the base station, it transmits RTK corrections using carrier phase measurements. Using this configuration, the rover can receive accurate correction data which allows them to achieve centimeter-level positioning accuracy.

The purpose of this group of experimental scenarios is to measure:

- To achieve positional accuracy when high quality RTK correction data delivered,
- The sensitivity of the vertical error,
- To measure the reliability of carrier-phase ambiguity resolution,
- The overall performance of positioning for the rovers within suitable RTK correction.

These experimental scenarios demonstrate the need to select high-quality hardware for the base station in RTK-enabled UAV precision landing systems.

7.2.3 Scenario Group 3: F9P Base Station Interchangeability Test

To evaluate the degree to which the F9P hardware modules are symmetric and interchangeable, a ZED-F9P module will be configured as the base station in surveying mode. Two F9P modules and an F9R module will be used as the rover modules.

With this configuration, it will be possible to evaluate:

- Consistency of identical hardware modules,
- Variations in performance due to receiver firmware or hardware tolerance issues,
- The stability of RTK correction generation when both the base and rover modules are comprised of identical multi-frequency modules.

Additionally, because the hardware modules will be alternated, the experiment will confirm that any observed differences in accuracy are not solely attributable to the specific hardware module acting as either the base or the rover.

7.2.4 Scenario Group 4: Alternate F9P Base Cross-Validation

A fourth validation scenario will repeat the interchangeability experiment using the alternate F9P unit as the base station. This validation will confirm that differences in the hardware modules do not create systematic biases in the evaluations.

Thus, this cross-validation will strengthen the robustness of the experiments by demonstrating that centimeter-level performance can be consistently achieved across identical receiver platforms.

7.2.5 Evaluation of Environmental Robustness

Each of the experimental groups will be performed under two environmental conditions:

1. Semi-obstructed laboratory-adjacent configuration with building shading effects,
2. Open-sky campus configuration with no obstructions blocking the view to the satellites.

This dual-environment approach allows for the quantification of:

- The impact of multipath effects on horizontal and vertical accuracy,
- The variability in convergence times,
- The ratio of RTK fixes available under partial obstruction,
- The performance gap between semi-obstructed and open-sky operations.

Because the hardware and correction parameters will be kept constant across environments, any performance variations will be attributed to the environmental propagation conditions rather than configuration variations.

7.3 Evaluation Metrics

A set of error metrics based on a unified approach has been developed to measure the quality of RTK positioning, for each experimental scenario. Horizontal, vertical and 3D root mean square errors (RMSE) are frequently used to quantify RTK positioning accuracy and the reliability of a system for UAV-RTK performance evaluations [43, 44]. The metrics have been calculated with respect to the GNSS observation timestamps recorded during the experiments.

7.3.1 Reference Coordinate Definition

In the case of static positioning trials, a reference coordinate $(x_{ref}, y_{ref}, z_{ref})$ was defined as the average value of all RTK-fixed observations, obtained during the open sky trial. This kind of mean-reference method is typically employed in RTK validation with limited or no access to survey-grade ground-truth data [43].

7.3.2 Horizontal Positioning Error (2D/H)

The horizontal positioning error, denoted as 2D/H in Tables, is the Euclidean distance between the measured and reference coordinates, projected into the horizontal plane:

$$E_{H,i} = \sqrt{(x_i - x_{ref})^2 + (y_i - y_{ref})^2} \tag{4}$$

The 2D/H value is the Root Mean Square Error (RMSE) of the horizontal deviations:

$$RMSE_H = \sqrt{\frac{1}{n}\sum_{i=1}^{n} E_{H,i}^2} \tag{5}$$

Horizontal RMSE is an accurate metric to use in the assessment of the accuracy of GNSS systems for UAV applications [44].

7.3.3 Vertical Positioning Error (2D/V)

The vertical positioning error, denoted as 2D/V, is the difference in elevation:

$$E_{V,i} = |z_i - z_{ref}| \tag{6}$$

The vertical RMSE is calculated as follows:

$$RMSE_V = \sqrt{\frac{1}{n}\sum_{i=1}^{n}(z_i - z_{ref})^2} \tag{7}$$

The assessment of vertical errors is critical in UAV precision landing because of the sensitivity of the descent phase [45].

7.3.4 Three-Dimensional Positioning Error (3D)

The three-dimensional positioning error accounts for both horizontal and vertical deviations:

$$E_{3D,i} = \sqrt{(x_i - x_{ref})^2 + (y_i - y_{ref})^2 + (z_i - z_{ref})^2} \tag{8}$$

The reported 3D metric is the RMSE of the full spatial deviation:

$$RMSE_{3D} = \sqrt{\frac{1}{n}\sum_{i=1}^{n} E_{3D,i}^2} \tag{9}$$

3D RMSE provides a simple way to represent the overall spatial accuracy of a system and is often used to summarize the results of RTK-UAV experimental validations [44]

7.3.5 RTK Solution Stability Metrics

In addition to the spatial accuracy, the stability of RTK solutions was evaluated by:

- **Fix Availability Ratio**

$$Availability = \frac{N_{fixed}}{N_{total}} \times 100\% \tag{10}$$

- **Convergence Time** Time that elapses between system startup and obtaining the first RTK-Fixed solution.
- **Fix-to-Float Transition Count** Number of times the RTK solution switches from RTK-Fixed to RTK-Float state.

The availability ratio and the time to convergence are widely accepted indicators of RTK reliability under dynamic and partially obstructed environments [46].

8 Results and Performance Analysis

A number of quantitative evaluations of the RTK-enabled UAV positioning framework for a UAV presented in this dissertation are provided in this chapter. The primary focus is on the positioning stability in static conditions and the RTK performance of the UAV in various environments and with different hardware configurations. Each result was calculated based on the evaluation parameters presented in Chapter 7: Horizontal RMSE (2D/H), Vertical RMSE (2D/V) and Three-Dimensional RMSE (3D).

All experiments were performed in two environments: Semi-obstructed Laboratory-Adjacent environment and Open-Sky Campus environment. The purpose of these experiments were to determine if there were any differences in the positioning accuracy that could be obtained from the different selections of hardware platforms, Correction Infrastructure, Quality of the Environmental Signal, or Integration Mode.

8.1 Static Positioning Results

Static Positioning Experiments were used to evaluate the ability of the system to provide repeatable coordinates, stable ambiguity resolution and degrade with environmental degradation. Static Positioning experiments isolate positioning errors due to UAV motion as the UAV does not move during static positioning experiments.

8.1.1 Performance under SAPOS Network Corrections

Table 2 provides the static positioning results under semi-obstructed conditions when SAPOS network corrections were used as the correction source.

From the experimental result, we found that the ZED-F9P unit gave the highest level of accuracy. It has a horizontal RMSE of 0.0141 m and a vertical RMSE of 0.0178 m, whereas the 3D error is 0.0227 m. From these observed values, it is clear that the carrier-phase corrections from the SAPOS network were successfully utilized and this RTK solution remained stable during our observation period.

The ZED-F9P module, which is the same F9P type, gave larger deviations. For this device, the horizontal RMSE was found at 0.0391 m and the vertical RMSE was at 0.0546 m, whereas a 3D error of 0.0672 m. Although the positioning accuracy is a bit lower than that obtained with our receiver, it is still within the expected range for RTK-enabled receivers operating in obstructed environments. A different behavior was observed for the ZED-F9R receiver, which gave a 3D RMSE of 1.666 m which is annotated to the left of the bar chart in Figure 21.

Table 2: Variation 1.1: SAPOS Network Correction in semi-obstructed environment

Rover	**Indoor (Semi-obstructed) (USB)**		
	2D/H	2D/V	3D
F9P (1st)	0.0141	0.0178	0.0227
F9P (2nd)	0.0391	0.0546	0.0672
F9R	1.1327	1.2219	1.6661

In Table 3 we have noted the positioning accuracy over different observation times containing 1 , 3 and 5 minutes after the devices start running. There is a clear trend that can be seen which shows that the accuracy improves as the observation time increases. In the case of ZED-F9P receiver, the horizontal RMSE decreased from 0.0755 m to 0.0484 m from one to five minutes. Similar improvements can be seen in the vertical and 3D error values, indicating that the RTK accuracy improves by times.

Table 3: Variation 1.2: GNSS Accuracy Comparison in Open-Sky (SAPOS Correction via Pixhawk)

Time	**Module**	**Fix Mode**	**2D/H [m]**	**2D/V [m]**	**3D [m]**
1 Min	F9P (1st)	3D/DGNSS/FLOAT	0.0755	0.1003	0.1256
	F9P (2nd)	3D/DGNSS/Fixed	0.0170	0.0275	0.0323
	F9R	3D/FLOAT	0.1377	0.1298	0.1893
3 Min	F9P (1st)	3D/DGNSS/FLOAT	0.0528	0.0667	0.0851
	F9P (2nd)	3D/DGNSS/FLOAT	0.0146	0.0165	0.0221
	F9R	3D/FLOAT	0.0523	0.0430	0.0677
5 Min	F9P (1st)	3D/DGNSS/FLOAT	0.0484	0.0636	0.0800
	F9P (2nd)	3D/DGNSS/FLOAT	0.0141	0.0140	0.0199
	F9R	3D/FLOAT	0.0291	0.0242	0.0379

The F9P receiver, which is another F9P device, gave the positioning accuracy of 0.0141 m and 0.0140 m at 5th minute, better than both of the other devices. The module's horizontal and vertical errors was approximately 0.014 m, which confirms that SAPOS corrections are capable of supporting centimeter-level positioning accuracy. It can be noted that the F9P module achieved a RTK Fixed with stable error levels within the first 180s. The 3D error observations over time in the case of open-sky when SAPOS was used as a base are shown in Figure 20.

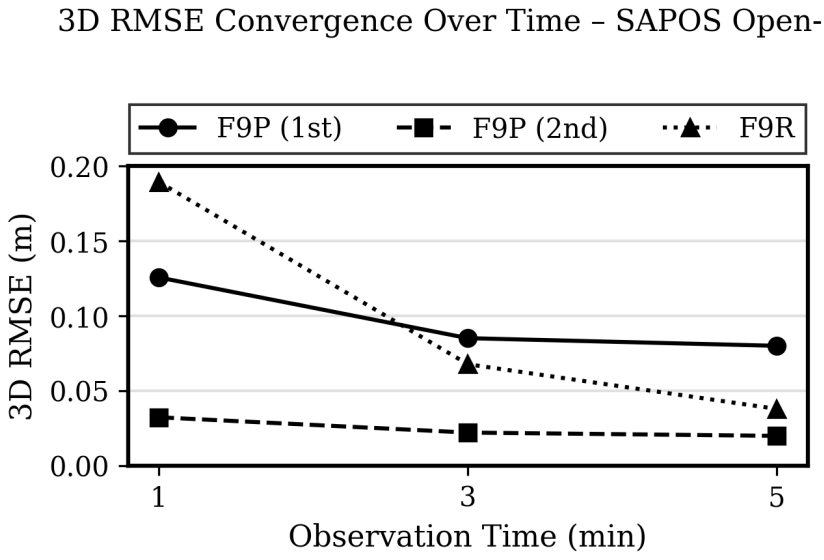

Figure 20: 3D RMSE convergence analysis over time [48].

The F9R receiver showed slightly better improvement over time; from 1 to 5 minutes, the horizontal RMSE decreased from 0.1377 m to 0.0291 m and same level of improvement was observed for vertical and 3D error observations.

If we compare in semi-obstructed and open-sky environments as can be seen in Figure 21, it is clear that Open-sky environments showed better accuracy improvement with the shortest times compared to the semi-obstructed, where we have waited more than 10 minutes to note down the better values possible.

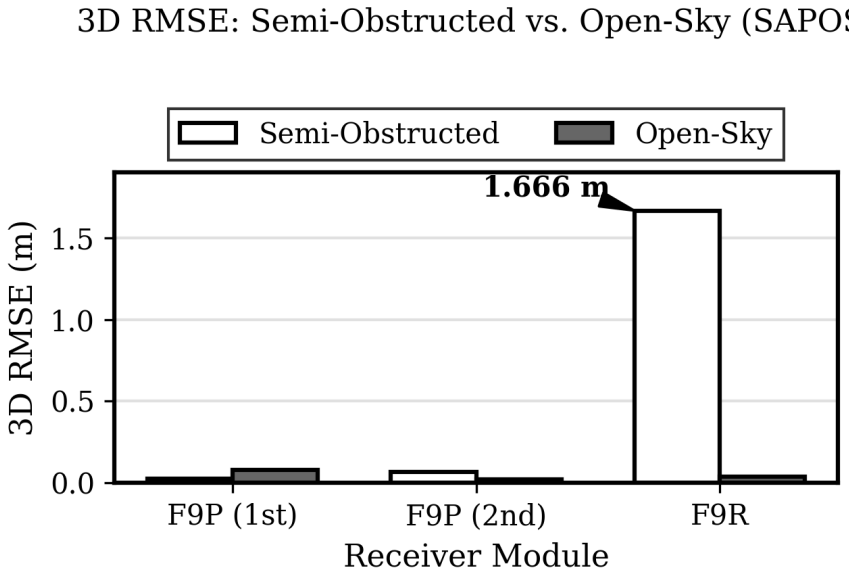

Figure 21: 3D RMSE comparison in different environments [48].

8.1.2 Performance under Here+ M8P Base Station Configuration

As presented in Table 4, we tested the Here+ M8P Base module where it was set up as the base station, and operating in Survey-In Mode. For this device, we have observed our base station at best possible survey accuracy of 17.5 meters in the semi-obstructed environment. Compared with the SAPOS configuration, for all the receivers, we observed a general decrease of accuracy. The F9P receiver showed a 3D error of 0.1719 m, where the other F9P achieved a slightly better result of 0.0916 m. We have found that the F9R receiver exhibited larger errors exceeding one meter in this semi-obstructed environment.

Table 4: Variation 2.1: Here+ M8P Base Station (Semi-obstructed) (Survey-In Mode)

Rover	**Indoor (Semi-obstructed) (USB)**		
	2D/H	**2D/V**	**3D**
F9P (1st)	0.1280	0.1147	0.1719
F9P (2nd)	0.0482	0.0779	0.0916
F9R	0.6088	1.3170	1.4509

During the open-sky testing as shown in Table 5, we tested our Here+ M8P Base at survey accuracy of 0.9999 meters and contributed to the improved performance of the

experimented devices. The F9P receiver achieved a 3D error of 0.0243 m after the device was kept for five minutes, verifying the fact that high precision can be achieved if we kept the GPS devices in sufficient satellite visibility. It was interesting to observe that the other F9P showed similar performance, which proves the fact that the primary limitation was the base station accuracy. Overall, we can say that Here+ M8P can deliver acceptable accuracy when kept in an open environment and its performance greatly depends on base level accuracy.

Table 5: Variation 2.2: GNSS Accuracy Comparison in Open-Sky (Here+ M8P Base)

Time	**Module**	**Fix Mode**	**2D/H [m]**	**2D/V [m]**	**3D [m]**
1 Min	F9P (1st)	3D/FLOAT	0.0225	0.0205	0.0305
	F9P (2nd)	3D/DGNSS/FLOAT	0.0619	0.0637	0.0888
	F9R	3D/FLOAT	0.1013	0.0934	0.1378
3 Min	F9P (1st)	3D/FLOAT	0.0210	0.0171	0.0271
	F9P (2nd)	3D/DGNSS/FLOAT	0.0224	0.0234	0.0324
	F9R	3D/FLOAT	0.0813	0.0634	0.1031
5 Min	F9P (1st)	3D/FLOAT	0.0178	0.0165	0.0243
	F9P (2nd)	3D/DGNSS/FLOAT	0.0141	0.0136	0.0196
	F9R	3D/FLOAT	0.0425	0.0348	0.0549

8.1.3 Base–Rover Interchangeability Analysis

The limitation we saw in the case of Here+ M8P base station, to overcome, there are two more bases we have tested in both semi-obstructed and open sky environments, which are shown in Table 6 for semi-obstructed case and both Table 7 and Table 8 for open-sky case.

To start the semi-obstructed testing, we kept our base station at best possible accuracy of 17.5 m. When we used the 1st variation of F9P as a base station, the second F9P rover achieved a 3D error of 0.0966 m, where the F9R showed higher errors exceeding one meter in both cases. Alternatively, when the second F9P was used as a base station, the first F9P had slightly less 3D error of 0.0399 m. These results prove that both F9P are suitable to use a base station and can contribute to the rover's centimeter level of accuracy.

Table 6: Variation 3.1 & 4.1: GNSS Accuracy Comparison: Indoor (Semi-obstructed) (USB)

Base Station	**Rover**	**2D/H**	**2D/V**	**3D**
F9P (1st)	F9P (2nd)	0.0458	0.0850	0.0966
	F9R	0.8968	1.1421	1.4521
F9P	F9P (1st)	0.0194	0.0349	0.0399
	F9R	0.5088	1.1170	1.2274

The findings above also confirmed when we did open-sky experiments. As can be seen in Table 7, when we tested first variation of F9P device as base station under survey accuracy

Table 7: Variation 3.2: Accuracy with F9P (1st) in Open Sky as Base Station

Time	Rover	Fix Mode	2D/H [m]	2D/V [m]	3D [m]
1 Min	F9P (2nd)	3D/FLOAT	0.0345	0.0362	0.0500
	F9R	3D/DGNSS/FLOAT	0.0850	0.1006	0.1317
3 Min	F9P (2nd)	3D/Fixed	0.0141	0.0100	0.0173
	F9R	3D/DGNSS/FLOAT	0.0172	0.0219	0.0278
5 Min	F9P (2nd)	3D/Fixed	0.0141	0.0132	0.0193
	F9R	3D/DGNSS/FLOAT	0.0141	0.0179	0.0228

of 0.9999 m, the another F9P achieved a 3D error of 0.0173m after three minutes passed and got RTK Fixed status.

Similarly, in Table 8 we also tested another F9P as base station with same surveyed accuracy of 0.9999 m, in this case both the F9P and F9R rovers have achieved RTK Fixed status within 3 minutes times. Thus, it is clear that Both F9P platforms are capable of symmetric base–rover operation with negligible systematic bias between devices. The interchangeability analysis demonstrates robustness and hardware compatibility within dual-frequency RTK configurations.

Table 8: Variation 4.2: Accuracy with F9P (2nd) in Open Sky as Base Station

Time	Rover	Fix Mode	2D/H [m]	2D/V [m]	3D [m]
1 Min	F9P (1st)	3D/FLOAT	0.0354	0.0535	0.0641
	F9R	3D/FLOAT	0.0320	0.0508	0.0600
3 Min	F9P (1st)	3D/FIXED	0.0141	0.0120	0.0186
	F9R	3D/FIXED	0.0141	0.0100	0.0173
5 Min	F9P (1st)	3D/FIXED	0.0141	0.0147	0.0204
	F9R	3D/FIXED	0.0141	0.0135	0.0195

In order to visually summarize the findings we have, Figure 22 descirbes how the 3D RMSE performance is identical for F9P base-rover pairs during the 3 and 5-minute observation periods. An almost identical error was observed when we swapped the roles of F9P (1st) and F9P (2nd) to verify the level of hardware consistency for these two devices within our system. This interchangeability analysis confirms that the positioning accuracy highly depends on the functionality of signal environment and satellite geometry instead of the individual device variance, ensuring reliable performance when used.

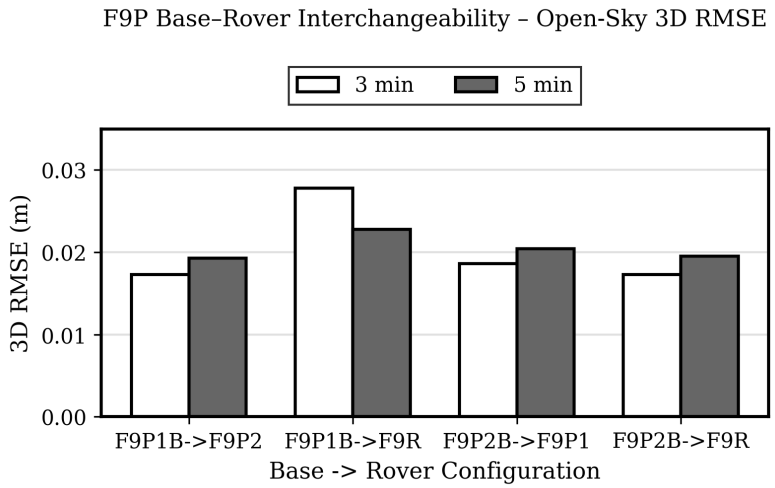

Figure 22: Base-Rover Interchangeability (F9P Pairs) [48].

8.1.4 Comprehensive Error Distribution Analysis

After evaluating all four types of base configurations, we are now going to analyze the error components across all semi-obstructed test scenarios. This analysis points out a clear distinction between horizontal and vertical accuracy limitations in the case of challenging GNSS environments. The Figure 23 illustrates how vertical errors significantly dominate the total errors in all the configurations. The F9R receiver showed more than 1m vertical errors for all the bases in the semi-obstructed environments. But, it is clear from the chart that the dual-frequency F9P modules can mitigate a substantial portion of these errors.

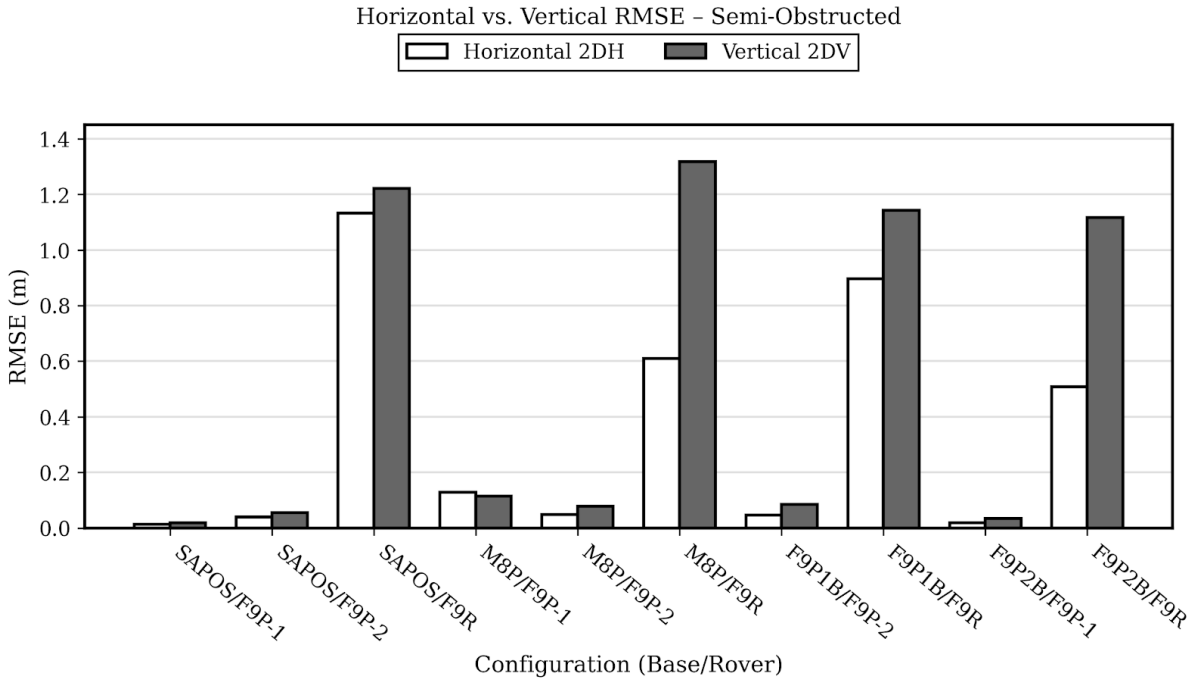

Figure 23: Horizontal vs. vertical RMSE for test configurations [48].

8.1.5 Environmental Impact Assessment

Across all static experiments, a consistent pattern emerged:

- Dual-frequency F9P modules in open-sky conditions provided centimeter-level accuracy.
- Laboratory conditions that were semi-obstructed resulted in a larger increase in vertical error compared to horizontal error.
- Receivers without a stable RTK-fixed generally exhibits a meter-level deviations.
- Infrastructure of correction system affected achievable precision.

The large error in height is due to multipath reflections as well as degradation of satellite geometry, both of which are much greater factors in estimating altitude.

8.2 Dynamic RTK Performance

Dynamic testing was used to study RTK stability while the UAV moved; specifically, dynamic testing evaluated the rover's performance under hover stabilization and controlled horizontal translation. The rover update rate was set to 5 Hz to measure short term positional variations.

8.2.1 Open-Sky Dynamic Performance

In the open sky environment, all F9P modules maintained a fixed position using RTK during both hovering and dynamic motion phases. The percentage of available fixes for these F9P modules exceeded 95 percent while they were in dynamic mode.

Analysis of trajectory smoothness indicated that there was little or no oscillation in the horizontal plane. The horizontal deviation mostly remained within the centimeter-level range and no prolonged transition into a floating state was noted.

On average, it took less than thirty seconds for each F9P module to achieve a RTK-fixed state from the start of the experiment. When a F9P module lost its RTK-fix due to loss of satellite signal (due to a short duration interruption), it regained RTK-fix state in seconds as soon as the satellite signal was restored.

The performance of the dual frequency RTK-modules under clear (open-sky) conditions demonstrates that dual frequency RTK-modules are capable of providing the same level of performance required for precision landing under similar conditions.

8.2.2 Semi-Obstructed Dynamic Performance

Under the laboratory adjacent (semi obstructed) conditions, some F9P modules had several fix to float transitions during the dynamic motion phase. Nearby structures caused

shading of satellites resulting in degradation of geometry and reduction in ability of the system to resolve ambiguities.

When an F9P module was in a float state, the horizontal deviation of the module increased, but the magnitude of increase was relatively small compared to the magnitude of increase in vertical deviations, which sometimes exceeded one decimeter. In addition, the F9P modules showed a rapid recovery back to RTK-fixed state.

The F9R module was found to be more sensitive to motion than the F9P module, since the F9R module experienced a higher number of fix-state transitions, and therefore had larger three dimensional dispersions.

8.2.3 Correction Source Influence in Dynamic Mode

No significant differences in the recovery times of the F9P modules were observed between the use of SAPOS network corrections versus locally generated corrections under open-sky conditions. However, under the semi obstructed conditions, longer recovery times were observed after a float transition when locally generated corrections were used.

As a result of this study, we can conclude that the effects of environmental conditions on RTK-module stability are much greater than the effects of correction sources under dynamic motion conditions when dual frequency hardware is being used.

8.3 Hardware Comparison Results

In a comparison of the technical capabilities of different GNSS hardware platforms, there are large differences in terms of the position stability of the system, its resistance against environmental influences and its dependence upon correction data. This study examines three different types of receivers (dual frequency modules ZED-F9P, single frequency modules ZED-F9R and Here+ M8P).

8.3.1 Dual-Frequency ZED-F9P Performance

For each of the three different measurement configurations tested, the dual frequency modules ZED-F9P were able to provide cm level horizontal accuracy for position determination under full sky conditions. For measurements using SAPOS correction data, horizontal root mean square errors (RMSE) were less than 0.02 m, and vertical RMSE was less than 0.04 m in the case of dynamic measurements.

Additional interchangeability testing of the base rover relationship between the two F9P modules clearly showed that the systematic deviations caused by each module were virtually identical. Swapping the role of the base station device between the two F9P modules resulted in no measurable positional offset, indicating an exceptionally high degree of hardware symmetry as well as consistency of the antenna characteristics of the two devices.

The results from the environmental sensitivity studies indicated that moderate degradation occurred when the devices were operated under semi-obscured laboratory conditions

due to the presence of multipath effects and partial shading. Even though there were some adverse environmental conditions present during the experiments, the maximum measured horizontal deviations were generally less than a decimeter. The measured vertical error was found to be significantly larger, however this is expected given the known sensitivity of RTK systems to the degradation of the satellite geometry.

In general, the dual frequency ZED-F9P modules provided:

- High RTK-Fixed availability,
- Rapid ambiguity convergence,
- Strong robustness under dynamic motion,
- Stable base–rover interchangeability.

These characteristics confirm suitability for precision landing operations requiring centimeter-level accuracy.

8.3.2 ZED-F9R Performance Characteristics

In comparison to the F9P modules, the ZED-F9R modules exhibited much larger variability. Horizontal performance improved in open-sky environment but overall positional accuracy lower than F9P modules. However, vertical error consistently exceeded one meter when the F9R units were tested under semi-obstructed conditions on several occasions.

As such, the F9R is intended to be used as part of a sensor-fusion application and may need optimized inertial integration to realize its highest level of performance. Pure GNSS positioning seems more prone to degradation due to environmental factors when no tight-coupled IMU fusion tuning has been performed on the system.

Additional dynamic testing demonstrated an increase in fix-to-float transitions when the F9R unit was operated near a laboratory. This indicates that both configuration and integration parameterizations have a significant influence on the stability of performance for the F9R unit.

8.3.3 CubePilot Here+ RTK GPS Performance

The CubePilot Here+ RTK GPS receiver achieved a centimeter-level offset in most open-sky configurations after the initial few minutes. Because of supporting carrier-phase positioning with satellite combinations like GPS and GLONASS, GPS and BeiDou, it is able to resolve integer ambiguities. Even if working under varying satellite visibility conditions, the receiver maintained a high level of positioning precision in most cases, except during obstructed lab situations, when the connected rovers gave a meter level of accuracy.

The experimental results clearly show that the CubePilot Here+ RTK GPS receiver can be used effectively for unmanned aerial vehicle (UAV) missions to acquire positioning accuracy close to a centimeter.

8.4 Precision Landing Accuracy

Precision landing accuracy was determined by measuring the difference between the UAV estimated position and the designated landing point during vertical descent phases.

8.4.1 Landing Stability under Open-Sky Conditions

When utilizing dual frequency RTK corrections and the F9P configuration during open-sky testing, the horizontal deviation at touch-down was within a few centimeters. In repeated tests, the final landing dispersion was less than 0.05 m.

As a result of the high fix availability ratio throughout the descent, there were minimal horizontal correction requirements placed upon the flight controller due to the ability of the RTK enabled GNSS to provide continuous centimeter level positioning.

Similarly, vertical stability remained well within acceptable tolerance limits. While there was a slight increase in the variability of the altitude estimates compared to the horizontal coordinates, no significant instability was noted during the final stages of the descent.

These results indicate that RTK enabled GNSS can provide sufficient accuracy to support autonomous landing in a controlled open-sky environment.

8.4.2 Landing Performance under Semi-Obstructed Conditions

During semi-obstructed testing, the precision landing accuracy was lower than that experienced during the open-sky testing. There were temporary fix-to-float transitions that caused the horizontal dispersion during the descent to increase.

Although the F9P modules normally quickly recovered RTK-Fixed status, the duration of the float periods introduced transient positional errors of larger than decimeter level magnitude.

The F9R modules showed even greater instability during the descent in the semi-obstructed environment. The increase in three-dimensional error translated into increased landing dispersion and decreased repeatability. The Here+ M8P also showed a bit less accuracy compared to other two devices.

8.4.3 Impact of Correction Infrastructure on Landing Accuracy

There were no differences in the landing accuracy achieved with SAPOS network corrections versus RTK corrections that were created on-site. However, the latency associated with network corrections may add time to recover from temporary float periods in environments where signal obstructions occur.

However, the effect of correction source selection was found to be secondary to the signal quality in the environment.

8.4.4 Operational Implications

The experimental results clearly demonstrate that the only way to achieve centimeter level landing accuracy is by meeting the following criteria:

- Dual-frequency RTK receiver deployment,
- Stable ambiguity resolution,
- Open-sky or minimally obstructed environment,
- High fix availability during descent.

In environments where significant amounts of multipath and/or signal blocking occur, RTK only solutions will likely require some form of complementary sensor fusion (e.g. vision based landing assistance) to provide reliable landing operations.

9 Discussion and Limitations

This chapter provides an interpretation of the experimental results from Chapter 8; and identifies the technical and methodological limitations of the RTK-enabled UAV positioning framework that was developed in this dissertation.

9.1 Discussion of Results

As shown by the experimental results, dual-frequency RTK receivers provided cm-level positioning accuracy under ideal (open sky) conditions. During both static and dynamic operations, the ZED-F9P modules consistently produced sub-2 cm horizontal root mean square error (RMSE), and maintained a high percentage of RTK-Fixed availability. These results demonstrate the success of carrier-phase based ambiguity resolution when the geometry of the satellite constellation and the quality of the correction infrastructure are maintained.

One of the most notable features of the results is the strong dependence of RTK performance on environment. In comparison to the horizontal errors, the vertical error under semi-obstructed laboratory-adjacent conditions increased much more rapidly. This increase in error is consistent with the sensitivity of the altitude estimation process to multipath reflections and reduced satellite geometry. The building-generated shading decreased the number of observable satellites and increased the probability of signal reflection, and therefore affected the stability of the ambiguity.

Another significant finding of this study is the demonstration of hardware symmetry of the ZED-F9P modules. The base-rover interchangeability test confirmed that there existed no detectable systematic difference between the base and rover versions of the ZED-F9P modules. Therefore, the same dual-frequency platform can perform reliably in either role without producing a measurable bias. This feature is particularly useful for modular UAV architectures.

Conversely, the ZED-F9R module had larger variability in its performance. Although it performed well under ideal (open-sky) conditions, the F9R module produced larger vertical dispersions and more frequent fix-to-float transitions under semi-obstructed dynamic conditions. Therefore, it appears that F9R may produce optimal performance if the tightly-coupled inertial sensor fusion is carefully tuned, which was outside the scope of the current evaluation.

The Here+ M8P single-frequency (L1-only) receiver produced meter-level deviations in some scenarios where satellite visibility was limited. For this kind of situations, the receiver was not able to maintain a stable RTK-Fixed status. As a result, it could not reliably solve for integer ambiguities, and therefore is not suitable for use in precision landing applications in semi-obstructed environment. These results clearly demonstrate the need for dual-frequency GNSS for UAV applications requiring cm-level positioning.

Additionally, the dynamic testing illustrated that environmental factors have a greater impact on the stability of RTK fixes than do the choice of correction source. Under ideal (open-sky) conditions, SAPOS network corrections and locally generated corrections resulted in similar performance. Conversely, under partially obstructed conditions, the

ability of the system to maintain continuous fixes and recover ambiguous solutions rapidly were the major determinants of the stability of the landing process.

Overall, these results illustrate that RTK-enabled UAV precision landing is technically possible in structured outdoor environments; however, the margin of performance decreases significantly in signal-degraded environments.

9.2 System Limitations

Although the results of this study were generally positive, there are some technical and methodological limitations to the work that must be noted.

Firstly, the study did not evaluate the effects of a diverse range of environments. The experiments were conducted in two distinct environments: a semi-obstructed laboratory-adjacent environment, and an open-sky university campus environment. Other environments, including urban canyon environments, densely vegetated environments, and high interference industrial environments, were not evaluated. Thus, the applicability of the results to highly complex urban environments is limited.

Secondly, the study was limited to evaluating the positioning capability of the GNSS system using only GNSS sensors, without considering other complementary sensor modalities, such as vision-based landing markers or tightly coupled inertial measurement unit (IMU) fusion. Although the evaluation was specifically targeted at isolating the performance of the RTK-only solution for analytical purposes, many operational systems that incorporate GNSS sensors also employ multi-modal sensing techniques to enhance their resistance to signal degradation.

Thirdly, the F9R module was primarily evaluated in GNSS-dominant mode, and little to no effort was made to calibrate the inertial sensor fusion component. Since F9R is intended for use in sensor fusion applications, it is reasonable to assume that its full performance potential may not have been realized in the course of this study.

Lastly, the latency of network corrections was not systematically evaluated. Although qualitative observations suggested that the delays associated with recovering fixes under semi-obstructed conditions were minimal, a quantitative evaluation of network correction latency was not within the scope of this dissertation.

Finally, the evaluation of landing accuracy was limited to controlled-descent trajectories. Wind disturbance, aggressive maneuvering, and emergency landing scenarios were not considered in the experimental design.

Thus, the aforementioned limitations identify avenues for future investigation, including:

- Evaluating the performance of the RTK-enabled UAV positioning framework in dense urban environments,
- Integrating vision-assisted landing capabilities into the RTK-enabled UAV positioning framework,
- Analyzing the tightly-coupled GNSS-IMU fusion performance of the ZED-F9P modules,

- Systematically evaluating the correction latency characteristics of SAPOS network corrections and locally generated corrections,
- Conducting long-duration reliability evaluations of the RTK-enabled UAV positioning framework.

Therefore, although the RTK-enabled UAV positioning framework demonstrated excellent performance in structured environments, additional research is needed to ensure the overall robustness of the framework in a broader range of operational environments.

10 Conclusion and Future Work

10.1 Conclusion

This dissertation project evaluated the ability of an RTK (Real-Time Kinematic) enabled UAV (Unmanned Aerial Vehicle) position estimation framework to enable precision landing applications based on an affordable multi-frequency receiver in a modular UAV platform. The main goal was to determine whether it is possible to achieve centimeter level GNSS (Global Navigation Satellite System) positioning using low-cost multi-frequency receivers, which have been incorporated into a modular UAV architecture.

The study started by providing a comprehensive overview of GNSS and RTK positioning theory, as well as the error mechanisms, carrier phase ambiguity resolution, and correction distribution mechanisms. Based upon this background, a full system architecture was defined that includes a dual-frequency GNSS receiver, correction infrastructure, flight controller interface, and structured real-time data logging framework.

Both open-sky and semi-obstructed environments, adjacent to the laboratory space, were used for experimental verification. Results indicated that the dual frequency ZED-F9P receiver successfully achieved centimeter level horizontal positioning accuracy under open-sky conditions. In addition, high RTK-Fixed availability, and fast convergence times validated the efficiency of the ambiguity resolution process in optimal signal environments.

The base-rover interchangeability analysis demonstrated that symmetrical operation of identical dual-frequency platforms does not introduce detectable systematic biases. This result supports the modular deployment of RTK-enabled UAV systems.

Results of the environmental sensitivity analysis show that positioning accuracy degradation in the vertical axis is greater than in the horizontal axis under conditions of multipath and satellite shading. The semi-obstructed experiments resulted in an increase in the number of fix-to-float transitions, and a larger standard deviation in the vertical axis, indicating the need to consider signal environment quality for reliable RTK operation.

The comparative hardware analysis demonstrated that multi-GNSS receivers capable of carrier phase measurements significantly outperform single-frequency receivers in terms of precision landing applications. The Here+ M8P module exhibited meter level positioning errors in some scenarios in indoor semi-obstructed environment, but in an open sky environment, having proper satellite visibility it gave a centimeter level of accuracy.

The data logging and processing framework employed in the study allowed for reproducibility, and statistical validation of each experiment's results. The use of real time acquisition, persistent storage to databases, back-end APIs, and visualization tools provided a robust experimental methodology for assessing the performance of RTK systems in UAVs.

Overall, the results of the thesis clearly indicate that RTK-enabled UAV precision landing is technologically viable under structured outdoor environments when high-quality dual frequency hardware and reliable correction sources are utilized. However, environmental constraints continue to represent significant factors affecting reliability.

10.2 Future Work

Although the framework that we developed has provided a set of validation approaches under controlled conditions, there are numerous opportunities for future research studies.

First of all, tight coupling of GNSS sensors with inertial measurement units or IMUs should be studied further. if we use more advanced fusion algorithms, it could potentially lead to improved positioning reliability under degraded signal conditions, or maybe during aggressive flight maneuvers.

Secondly, vision-assisted landing systems can help RTK positioning. By utilizing GNSS-based absolute positioning with visual markers may enhance landing precision in environments with partial satellite obstruction like our semi-obstructed drone lab conditions.

Thirdly, further experiments in case of complex urban canyon environments will be necessary. The dense infrastructure present in these environments creates situations like extreme multipath and signal blocking effects, none of which were thoroughly tested in during study.

Fourthly, correction latency analysis should be conducted in a quantitative manner. By determining the relationship between network correction latency and ambiguity resolution stability, there can be a better understanding of the performance limitations inherent in case of dynamic operation.

Fifthly, long duration reliability tests under various weather conditions will help us to assess system robustness over extended operating periods.

Sixth, future work could examine the integration of autonomous hangars with cloud-based fleet management architectures, allowing for scalable deployment of RTK-enabled UAV fleets.

In summary we can say that, my thesis has provided a comprehensive experimental and methodological basis for RTK-based UAV precision landing systems. The results shown herein show the potential of cost effective dual frequency GNSS hardware to achieve centimeter level accuracy, while also illustrating the environmental and integration challenges that must be resolved in order to facilitate large scale operational deployment of RTK-enabled UAVs.

Bibliography

[1] L. Obaid *et al.*, “State-of-the-art review of unmanned aerial vehicles (UAVs) and artificial intelligence (AI) for traffic and safety analyses: Recent progress, applications, challenges, and opportunities,” *Transp. Res. Interdiscip. Perspect.*, vol. 33, p. 101591, Sep. 2025, doi: 10.1016/j.trip.2025.101591.

[2] T. Suzuki, D. Inoue and Y. Amano, "Robust UAV Position and Attitude Estimation using Multiple GNSS Receivers for Laser-based 3D Mapping," 2019 IEEE/RSJ International Conference on Intelligent Robots and Systems (IROS), Macau, China, 2019, pp. 4402-4408, doi: 10.1109/IROS40897.2019.8967894

[3] H. Kim, C.-U. Hyun, H.-D. Park, and J. Cha, “Image Mapping Accuracy Evaluation Using UAV with Standalone, Differential (RTK), and PPP GNSS Positioning Techniques in an Abandoned Mine Site,” *Sensors*, vol. 23, no. 13, p. 5858, Jun. 2023, doi: 10.3390/s23135858.

[4] A. D. Jordan, M. Rydalch, T. McLain, and M. Williamson, “Precision Maritime Localization and Landing with Real-time Kinematic GNSS,” in *Proc. AIAA SCITECH 2023 Forum*, Jan. 2023, Paper AIAA 2023-0488, doi: 10.2514/6.2023-0488.

[5] S. Punzet and T. F. Eibert, “Impact of Additional Antenna Groundplanes on RTK-GNSS Positioning Accuracy of UAVs,” *Adv. Radio Sci.*, vol. 20, pp. 23–30, May 2023, doi: 10.5194/ars-20-23-2023.

[6] L. Tavasci *et al.*, “Reliability of Real-Time Kinematic Positioning for UAVs,” *Sensors*, vol. 24, no. 18, p. 6096, Sep. 2024, doi: 10.3390/s24186096.

[7] Z. Liu, Y. Lv, G. Chen, L. Zhao, F. Wei, and Y. Pan, “Analysis of real-time kinematic positioning of UAV based on BDS-3 PPP-B2b service,” *Adv. Space Res.*, 2025, doi: 10.1016/j.asr.2025.09.070.

[8] M. N. Alkan, “High-Precision UAV Photogrammetry with RTK GNSS: Eliminating Ground Control Points,” *Hittite J. Sci. Eng.*, vol. 11, no. 4, pp. 139–147, 2024, doi: 10.17350/HJSE19030000341.

[9] V. Hamza *et al.*, “Observations and positioning quality of low-cost GNSS receivers: a review,” *GPS Solut.*, vol. 28, no. 3, p. 149, May 2024, doi: 10.1007/s10291-024-01686-8.

[10] F. R. Matzke *et al.*, “Addressing GNSS Vulnerabilities in AAM: A Multi-Modal UAV Testbed for Redundant and Reliable Navigation,” *Int. Arch. Photogramm. Remote Sens. Spat. Inf. Sci.*, vol. XLVIII-2-W11-2025, pp. 211–218, 2025, doi: 10.5194/isprs-archives-XLVIII-2-W11-2025-211-2025.

[11] H. Wu, W. Wang, T. Wang, and S. Suzuki, “High-precision landing on a moving platform based on drone vision using YOLO algorithm,” *Drones*, vol. 9, no. 4, p. 261, Apr. 2025, doi: 10.3390/drones9040261.

[12] A. E. Kianfar, “Ultra-wideband based positioning systems for harsh mining environment,” Dr. Ing. thesis, Dept. Comput. Sci., RWTH Aachen Univ., Aachen, Germany, 2022, doi: 10.13140/RG.2.2.22511.92329.

[13] P. J. G. Teunissen, "The least-squares ambiguity decorrelation adjustment: A method for fast GPS integer ambiguity estimation," *J. Geod.*, vol. 70, no. 1–2, pp. 65–82, Nov. 1995, doi: 10.1007/BF00863419.

[14] G. Wübbena, A. Bagge, and M. Schmitz, "Reference station network based RTK systems – concepts and progress," *J. Glob. Positioning Syst.*, vol. 2, no. 1, pp. 20–31, Jun. 2003, doi: 10.5081/jgps.2.1.20.

[15] C. Rizos, "Network RTK research and implementation – a geodetic perspective," *J. Glob. Positioning Syst.*, vol. 1, no. 2, pp. 144–150, Dec. 2002, doi: 10.5081/jgps.1.2.144.

[16] R. Odolinski, P. J. G. Teunissen, and D. Odijk, "Multi-GNSS RTK positioning: Performance analysis," in *Proc. IGNSS Conf. 2015*, Gold Coast, QLD, Australia, Jul. 2015, pp. 1–15.

[17] X. Mi *et al.*, "Multi-GNSS RTK positioning with integer ambiguity resolution: From double-differenced to single-differenced," *J. Glob. Positioning Syst.*, vol. 19, no. 1, p. 11, Dec. 2021, doi: 10.1186/s41239-021-00263-x.

[18] D. L. Wu, J. J. Yin, and X. L. Zhang, "Research on Virtual Reference Station (VRS) technology and differential correction information," *J. Phys.: Conf. Ser.*, vol. 1907, no. 1, p. 012015, May 2021, doi: 10.1088/1742-6596/1907/1/012015.

[19] S. Alissa *et al.*, "Low bandwidth network-RTK correction dissemination for high accuracy maritime navigation," *TransNav, Int. J. Mar. Navig. Saf. Sea Transp.*, vol. 15, no. 2, pp. 355–362, Jun. 2021, doi: 10.12716/1001.15.02.10.

[20] B. Li *et al.*, "Ambiguity resolution for smartphone GNSS precise positioning: Effect factors and performance," *J. Geod.*, vol. 96, no. 9, p. 65, Sep. 2022, doi: 10.1007/s00190-022-01655-y.

[21] Y. Jiang, Y. Gao, W. Ding, F. Liu, and Y. Gao, "An improved ambiguity resolution algorithm for smartphone RTK positioning," *Sensors*, vol. 23, no. 11, p. 5292, Jun. 2023, doi: 10.3390/s23115292.

[22] J. Hu, D. Yi, and S. Bisnath, "Towards GNSS ambiguity resolution for smartphones in realistic environments: Characterization of smartphone ambiguities with RTK, PPP, and PPP-RTK," in *Proc. 36th Int. Tech. Meeting Satellite Div. Inst. Navigation (ION GNSS+ 2023)*, Denver, CO, USA, Sep. 2023, pp. 2533–2544, doi: 10.33012/2023.19285.

[23] G. Boquet, X. Vilajosana, and B. Martinez, "Feasibility of providing high-precision GNSS correction data through non-terrestrial networks," *IEEE Trans. Instrum. Meas.*, vol. 73, pp. 1–11, Sep. 2024, Art. no. 5503915, doi: 10.1109/TIM.2024.3453319.

[24] W. Miao, C. Xu, Y. Jiang, Y. Gao, and Y. Yao, "The superiority of multi-GNSS L5/E5a/B2a frequency signals in smartphones: Stochastic modelling, ambiguity resolution and RTK positioning," *IEEE Internet Things J.*, vol. 10, no. 8, pp. 6810–6823, Apr. 2023, doi: 10.1109/JIOT.2022.3228945.

[25] H. Huang, M. Zhou, H. Yan, and L. Yuan, "Analysis of the dynamic characteristics of a suspension bridge based on RTK-GNSS measurement combining EEMD and wavelet packet technique," *Sensors*, vol. 18, no. 6, p. 1834, Jun. 2018, doi: 10.3390/s18061834.

[26] B. Eissfeller, D. Dötterböck, S. Junker, and C. Stöber, "Online GNSS data processing – status and future developments," in *Proc. 53rd Photogramm. Week*, Stuttgart, Germany, Sep. 2011, pp. 111–120.

[27] ArduSimple, "simpleRTK2B ZED-F9P product page," [Online]. Available: https://www.ardusimple.com/product/simplertk2b/. Accessed: Feb. 19, 2025.

[28] u-blox, "ZED-F9P: High precision GNSS module data sheet," u-blox AG, Thalwil, Switzerland, Doc. UBX-18010802, 2022. [Online]. Available: https://www.u-blox.com/en/product/zed-f9p-module.

[29] CubePilot, "Here+ V2 User Manual," [Online]. Available: https://docs.cubepilot.org/user-guides/here+/here+v2-user-manual. Accessed: Feb. 19, 2025.

[30] Holybro, "H-RTK F9P GNSS positioning set," [Online]. Available: https://holybro.com/products/h-rtk-f9p. Accessed: Feb. 19, 2025.

[31] ArduSimple, "WiFi NTRIP master," [Online]. Available: https://www.ardusimple.com/product/wifi-ntrip-master/. Accessed: Feb. 19, 2025.

[32] Holybro, "Pixhawk 4 autopilot," [Online]. Available: https://holybro.com/products/pixhawk-4. Accessed: Feb. 19, 2025.

[33] AdV, "SAPOS – Satellite positioning service of Germany," Working Committee of the Surveying Authorities of the Laender of the Federal Republic of Germany (AdV), [Online]. Available: https://www.adv-online.de/Products/SAPOS/. Accessed: Feb. 19, 2025.

[34] SAPOS Hessen, "SAPOS HEPS service description," Hessian State Office for Land Management and Geoinformation (HVBG), [Online]. Available: https://sapos.hvbg.hessen.de/service.php. Accessed: Feb. 19, 2025.

[35] ArduSimple, "How to configure u-blox ZED-F9P," ArduSimple Tutorials, [Online]. Available: https://www.ardusimple.com/how-to-configure-ublox-zed-f9p/. Accessed: Feb. 19, 2025.

[36] ArduSimple, "How to configure simpleRTK2B as static base station," ArduSimple Tutorials, [Online]. Available: https://www.ardusimple.com/how-to-configure-simplertk2b-as-static-base-station/. Accessed: Feb. 19, 2025.

[37] ArduSimple, "How to configure simpleRTK2B Basic Starter Kit (ZED-F9P) and connect it to ArduPilot," ArduSimple Tutorials, [Online]. Available: https://www.ardusimple.com/how-to-configure-simplertk2b-basic-starter-kit-zed-f9p-module-and-connect-it-to-ardupilot-to-get-centimeter-accurate-gps-location/. Accessed: Feb. 19, 2025.

[38] Tavasci, Luca, Francesco Nex, and Stefano Gandolfi. 2024. "Reliability of Real-Time Kinematic (RTK) Positioning for Low-Cost Drones' Navigation across Global Navigation Satellite System (GNSS) Critical Environments" Sensors 24, no. 18: 6096. https://doi.org/10.3390/s24186096

[39] Czyża, S., Szuniewicz, K., Kowalczyk, K., Dumalski, A., Ogrodniczak, M., & Zieleniewicz, Ł. (2023). Assessment of Accuracy in Unmanned Aerial Vehicle (UAV) Pose Estimation with the REAL-Time Kinematic (RTK) Method on the Example of DJI Matrice 300 RTK. Sensors, 23(4), 2092. https://doi.org/10.3390/s23042092

[40] B. Zhou, Y. Li, W. Shi and C. Yuan, "An Acoustic-Aided RTK UAV Positioning Method for Occluded Environments," in IEEE Access, vol. 14, pp. 13330-13347, 2026, doi: 10.1109/ACCESS.2026.3656895.

[41] J. H. Jepsen, F. Gunnarsson, R. Wen, J. Wase and K. Jensen, "Experimental Results of Utilizing the 3GPP LTE Positioning Protocol for Providing RTK Reference Data to High-Accuracy UAV Operations," 2024 International Conference on Unmanned Aircraft Systems (ICUAS), Chania - Crete, Greece, 2024, pp. 53-60, doi: 10.1109/ICUAS60882.2024.10556963.

[42] Tavasci, Luca, Francesco Nex, and Stefano Gandolfi. 2024. "Reliability of Real-Time Kinematic (RTK) Positioning for Low-Cost Drones' Navigation across Global Navigation Satellite System (GNSS) Critical Environments" Sensors 24, no. 18: 6096. https://doi.org/10.3390/s24186096

[43] Cățeanu, Mihnea, and Maria Alexandra Moroianu. 2024. "Performance Evaluation of Real-Time Kinematic Global Navigation Satellite System with Survey-Grade Receivers and Short Observation Times in Forested Areas" Sensors 24, no. 19: 6404. https://doi.org/10.3390/s24196404

[44] Tavasci, Luca, Francesco Nex, and Stefano Gandolfi. 2024. "Reliability of Real-Time Kinematic (RTK) Positioning for Low-Cost Drones' Navigation across Global Navigation Satellite System (GNSS) Critical Environments" Sensors 24, no. 18: 6096. https://doi.org/10.3390/s24186096

[45] D. Heo, H. Hwang, J. Choi and S. Choi, "Leveraging GNSS Accuracy With a Barometer," in IEEE Sensors Journal, vol. 25, no. 13, pp. 25754-25767, 1 July1, 2025, doi: 10.1109/JSEN.2025.3568843.

[46] G. Boquet, X. Vilajosana, and B. Martinez, "Experimental Validation of Duty-Cycled RTK GNSS Positioning for Low-Power High-Precision Quasi-Static Monitoring," IEEE Transactions on Aerospace and Electronic Systems, vol. PP, no. 99, pp. 1–14, Jan. 2026, doi: 10.1109/TAES.2026.3662317.

[47] F. Silva, "ECEF position accuracy and reliability: Continent scale differential GNSS approaches (Phase C Report)," 2019.

[48] Google, "Gemini," Google LLC, 2025. [Online]. Available: https://gemini.google.com. [Accessed: Mar. 2025].

Bibliography from TUC

[TUC1] B. Battseren, S. Saleh, M. S. Harras, D. A. Orjuela Aguirre, and W. Hardt, "Tree detection and localization approach for UAV-based forest inspection," *Embedded Self Organizing Systems*, vol. 9, no. 3, pp. 73–81, 2022.

[TUC2] Z. Bayasgalan, U. Tudevdagva, A. Sukhbaatar, and W. Hardt, "Top inspection and monitoring of HV power line towers damage by UAV," in *Proc. Int. Conf. Technol. Policy Energy Electr. Power (ICT-PEP)*, 2021, pp. 248–252, doi: 10.1109/ICT-PEP53949.2021.9601091.

[TUC3] R. Harradi, A. Heller, and W. Hardt, "Decentralized UAV hangar: A study for water rescue missions," in *Proc. 2024 Int. Symp. Comput. Sci. Educ. Technol. (ISCSET)*, 2024, doi: 10.1109/ISCSET58624.2024.10807887.

[TUC4] R. Harradi, A. Heller, J. Roth, and W. Hardt, "MAVLink UAV hangar communication based on a cloud architecture," in *Proc. 66th Int. Symp. Electron. Mar. (ELMAR)*, Zadar, Croatia, Sep. 2024, pp. 301–305, doi: 10.1109/ELMAR62909.2024.10694538.

[TUC5] F. Kilic, M. Hassan, and W. Hardt, "Prototype for multi-UAV monitoring/control system using WebRTC," *Drones*, vol. 8, no. 10, p. 551, Oct. 2024, doi: 10.3390/drones8100551.

[TUC6] U. Tudevdagva, B. Battseren, W. Hardt, S. Blokzyl, and M. Lippmann, "Unmanned aerial vehicle-based fully automated inspection system for high voltage transmission lines," in *Proc. 12th Int. Forum Strategic Technol. (IFOST)*, Ulsan, South Korea, 2017, pp. 300–305.

Chemnitzer Informatik-Berichte

In der Reihe der Chemnitzer Informatik-Berichte sind folgende Berichte erschienen:

CSR-24-01 Seyhmus Akaslan, Ariane Heller, Wolfram Hardt, Hardware-Supported Test Environment Analysis for CAN Message Communication, Juni 2024, Chemnitz

CSR-24-02 S. M. Rizwanur Rahman, Wolfram Hardt, Image Classification for Drone Propeller Inspection using Deep Learning, August 2024, Chemnitz

CSR-24-03 Sebastian Pettke, Wolfram Hardt, Ariane Heller, Comparison of maximum weight clique algorithms, August 2024, Chemnitz

CSR-24-04 Md Shoriful Islam, Ummay Ubaida Shegupta, Wolfram Hardt, Design and Development of a Predictive Learning Analytics System, August 2024, Chemnitz

CSR-24-05 Sopuluchukwu Divine Obi, Ummay Ubaida Shegupta, Wolfram Hardt, Development of a Frontend for Agents in a Virtual Tutoring System, August 2024, Chemnitz

CSR-24-06 Saddaf Afrin Khan, Ummay Ubaida Shegupta, Wolfram Hardt, Design and Development of a Diagnostic Learning Analytics System, August 2024, Chemnitz

CSR-24-07 Túlio Gomes Pereira, Wolfram Hardt, Ariane Heller, Development of a Material Classification Model for Multispectral LiDAR Data, August 2024, Chemnitz

CSR-24-08 Sumanth Anugandula, Ummay Ubaida Shegupta, Wolfram Hardt, Design and Development of a Virtual Agent for Interactive Learning Scenarios, September 2024, Chemnitz

CSR-25-01 Md. Ali Awlad, Hasan Saadi Jaber Aljzaere, Wolfram Hardt, AUTOSAR Software Component for Atomic Straight Driving Patterns, März 2025, Chemnitz

CSR-25-02 Billava Vasantha Monisha, Hasan Saadi Jaber Aljzaere, Wolfram Hardt, Automotive Software Component for QT Based Car Status Visualization, März 2025, Chemnitz

CSR-25-03 Zahra Khadivi, Batbayar Battseren, Wolfram Hardt, Acoustic-Based MAV Propeller Inspection, Mai 2025, Chemnitz

Chemnitzer Informatik-Berichte

CSR-25-04 Tripti Kumari Shukla, Ummay Ubaida Shegupta, Wolfram Hardt, Time Management Tool Development to Support Self-regulated Learning, August 2025, Chemnitz

CSR-25-05 Ambu Babu, Ummay Ubaida Shegupta, Wolfram Hardt, Development of a Retrieval Model based Backend of a Tutoring Agent, August 2025, Chemnitz

CSR-25-06 Shahid Ismail, Ummay Ubaida Shegupta, Wolfram Hardt, Development of a Generative Model based Backend of Tutoring Agent, August 2025, Chemnitz

CSR-25-07 Chaitanya Sravanthi Akula, Ummay Ubaida Shegupta, Wolfram Hardt, Integration of Learning Analytics into the ARC-Tutoring Workbench, August 2025, Chemnitz

CSR-25-08 Jörn Roth, Reda Harradi, Wolfram Hardt, Implementation of a Path Planning Algorithm for UAV Navigation, Dezember 2025, Chemnitz

CSR-25-09 Alhassan Khalil, Reda Harradi, Stephan Rupf, Wolfram Hardt, Development of an Automation Framework for 1D Measurement, Dezember 2025, Chemnitz

CSR-26-01 Vismay Gunda, Shadi Saleh, Wolfram Hardt, Cloud-Based AI Solutions for Ensuring Data Quality in Predictive Models, Februar 2026, Chemnitz

CSR-26-02 Sami Mansoor Alavi, Shadi Saleh, Wolfram Hardt, Continuous Integration for Cloud-Based Swarm Farming Applications, Februar 2026, Chemnitz

CSR-26-03 Sarah Onyinyechi Obasi, Shadi Saleh, Wolfram Hardt, Cloud-Based AI for Data Completeness Analysis and Improvement in Predictive Modeling, März 2026, Chemnitz

CSR-26-04 Atul Chandra Nath, Reda Harradi, Wolfram Hardt, GPS-based UAV Precision Landing, April 2026, Chemnitz

Chemnitzer Informatik-Berichte

ISSN 0947-5125

Herausgeber: Fakultät für Informatik, TU Chemnitz
Straße der Nationen 62, D-09111 Chemnitz